

1 **Robust, flexible, and scalable tests for**

2 **Hardy-Weinberg Equilibrium across**

3 **diverse ancestries**

4

5 Alan M. Kwong<sup>1</sup>, Thomas W. Blackwell<sup>1</sup>, Jonathon LeFaive<sup>1</sup>, Mariza de Andrade<sup>2</sup>, John Barnard<sup>3</sup>,  
6 Kathleen C. Barnes<sup>4</sup>, John Blangero<sup>5</sup>, Eric Boerwinkle<sup>6,7</sup>, Esteban G. Burchard<sup>8,9</sup>, Brian E. Cade<sup>10,11</sup>,  
7 Daniel I. Chasman<sup>12</sup>, Han Chen<sup>6,13</sup>, Matthew P. Conomos<sup>14</sup>, L. Adrienne Cupples<sup>15,16</sup>, Patrick T.  
8 Ellinor<sup>17,18</sup>, Celeste Eng<sup>9</sup>, Yan Gao<sup>19</sup>, Xiuqing Guo<sup>20</sup>, Marguerite Ryan Irvin<sup>21</sup>, Tanika N. Kelly<sup>22</sup>,  
9 Wonji Kim<sup>23</sup>, Charles Kooperberg<sup>24</sup>, Steven A. Lubitz<sup>17,18</sup>, Angel C. Y. Mak<sup>9</sup>, Ani W. Manichaikul<sup>25</sup>,  
10 Rasika A. Mathias<sup>26</sup>, May E. Montasser<sup>27</sup>, Courtney G. Montgomery<sup>28</sup>, Solomon Musani<sup>29</sup>,  
11 Nicholette D. Palmer<sup>30</sup>, Gina M. Peloso<sup>15</sup>, Dandi Qiao<sup>23</sup>, Alexander P. Reiner<sup>24</sup>, Dan M. Roden<sup>31</sup>,  
12 M. Benjamin Shoemaker<sup>32</sup>, Jennifer A. Smith<sup>33</sup>, Nicholas L. Smith<sup>34,35,36</sup>, Jessica Lasky Su<sup>23</sup>,  
13 Hemant K. Tiwari<sup>37</sup>, Daniel E. Weeks<sup>38</sup>, Scott T. Weiss<sup>23</sup>, NHLBI Trans-Omics for Precision Medicine  
14 (TOPMed) Consortium, TOPMed Analysis Working Group, Laura J. Scott<sup>1</sup>, Albert V. Smith<sup>1</sup>,  
15 Gonçalo R. Abecasis<sup>1</sup>, Michael Boehnke<sup>1</sup>, Hyun Min Kang<sup>1,\*</sup>

16

17 1 - Department of Biostatistics and Center for Statistical Genetics, University of Michigan, Ann  
18 Arbor, MI 48109; 2 - Mayo Clinic, Rochester, MN 55905; 3 - Department of Quantitative Health  
19 Sciences, Lerner Research Institute, Cleveland Clinic, Cleveland, OH 44106; 4 - Department of  
20 Medicine, Anschultz Medical Campus, University of Colorado, Aurora, CO 80045; 5 -  
21 Department of Human Genetics and South Texas Diabetes and Obesity Institute, University of  
22 Texas Rio Grande Valley School of Medicine, Brownsville, TX 78520; 6 - Human Genetics Center,  
23 Department of Epidemiology, Human Genetics and Environmental Sciences, School of Public  
24 Health, The University of Texas Health Science Center at Houston, Houston, TX 77030; 7 -  
25 Human Genome Sequencing Center, Baylor College of Medicine, Houston, TX 77030; 8 -  
26 Department of Bioengineering and Therapeutic Sciences, University of California San Francisco,  
27 San Francisco, CA 94143; 9 - Department of Medicine, University of California San Francisco,  
28 San Francisco, CA 94143; 10 - Division of Sleep and Circadian Disorders, Brigham and Women's  
29 Hospital, Boston, MA 02115; 11 - Division of Sleep Medicine, Harvard Medical School, Boston,  
30 MA 02115; 12 - Division of Preventive Medicine, Brigham and Women's Hospital, Boston, MA  
31 02115; 13 - Center for Precision Health, School of Public Health and School of Biomedical

32 Informatics, The University of Texas Health Science Center at Houston, Houston, TX 77030; 14 -  
33 Department of Biostatistics, University of Washington, Seattle, WA 98195; 15 - Department of  
34 Biostatistics, Boston University School of Public Health, Boston, MA 02118; 16 - Framingham  
35 Heart Study, Framingham, MA 01702; 17 - Cardiovascular Research Center, Massachusetts  
36 General Hospital, Boston, MA 02114; 18 - Cardiovascular Disease Initiative, The Broad Institute  
37 of MIT and Harvard, Cambridge, MA 02124; 19 - Department of Physiology and Biophysics,  
38 University of Mississippi Medical Center, Jackson, MS 39216; 20 - The Institute for Translational  
39 Genomics and Population Sciences, Department of Pediatrics, The Lundquist Institute at  
40 Harbor-UCLA Medical Center, Torrance, CA, 90502; 21 - Department of Epidemiology, School of  
41 Public Health, University of Alabama at Birmingham, Birmingham, AL 35294; 22 - Department of  
42 Epidemiology, Tulane University, New Orleans, LA 70112; 23 - Channing Division of Network  
43 Medicine, Department of Medicine, Brigham and Women's Hospital and Harvard Medical  
44 School, Boston, MA 02115; 24 - Fred Hutchinson Cancer Research Center, Seattle, WA 98109;  
45 25 - Center for Public Health Genomics, Department of Public Health Sciences, University of  
46 Virginia, Charlottesville, VA 22908; 26 - GeneSTAR Research Program and Division of Allergy and  
47 Clinical Immunology, Department of Medicine, Johns Hopkins University, Baltimore, MD 21205;  
48 27 - Division of Endocrinology, Diabetes and Nutrition, Department of Medicine, University of  
49 Maryland School of Medicine, Baltimore, MD 21201; 28 - Sarcoidosis Research Unit, Genes and  
50 Human Disease Research Program, and Quantitative Analysis Core, Oklahoma Medical Research  
51 Foundation, Oklahoma City, OK 73104; 29 - Jackson Heart Study, University of Mississippi  
52 Medical Center, Jackson, MS 39216; 30 - Department of Biochemistry, Wake Forest School of  
53 Medicine, Winston-Salem, NC 27157; 31 - Departments of Medicine, Pharmacology, and  
54 Biomedical Informatics, Vanderbilt University Medical Center, Nashville, TN 37232; 32 -  
55 Department of Medicine, Vanderbilt University Medical Center, Nashville, TN 37232; 33 -  
56 Department of Epidemiology, School of Public Health, University of Michigan, Ann Arbor, MI  
57 48109; 34 - Department of Epidemiology, University of Washington, Seattle WA 98195; 35 -  
58 Kaiser Permanente Washington Health Research Institute, Kaiser Permanente Washington,  
59 Seattle WA 98101; 36 - Seattle Epidemiologic Research and Information Center, Office of  
60 Research and Development, Department of Veterans Affairs, Seattle WA 98108; 37 -  
61 Department of Biostatistics, School of Public Health, University of Alabama at Birmingham,  
62 Birmingham, AL 35294; 38 - Departments of Human Genetics and Biostatistics, Graduate School  
63 of Public Health, University of Pittsburgh, PA 15261

64 \*Corresponding author: Center for Statistical Genetics and the Department of Biostatistics, University of  
65 Michigan, Ann Arbor, MI 48109. E-mail: hmkang@umich.edu

66

67

# 68 HWE tests for diverse ancestries

## 69 KEYWORDS

70 population structure; principal components analysis; next-generation sequencing; genotype

71 likelihoods

72

## 73 CORRESPONDING AUTHOR

74 Hyun Min Kang

75 Department of Biostatistics

76 University of Michigan School of Public Health

77 1415 Washington Heights

78 Ann Arbor, MI 48109

79 Phone: 734-647-1980

80 E-mail: [hmkang@umich.edu](mailto:hmkang@umich.edu)

81

## 82 ABSTRACT

83 Traditional Hardy-Weinberg equilibrium (HWE) tests (the  $\chi^2$  test and the exact test) have long  
84 been used as a metric for evaluating genotype quality, as technical artifacts leading to incorrect  
85 genotype calls often can be identified as deviations from HWE. However, in datasets comprised  
86 of individuals from diverse ancestries, HWE can be violated even without genotyping error,  
87 complicating the use of HWE testing to assess genotype data quality. In this manuscript, we  
88 present the Robust Unified Test for HWE (RUTH) to test for HWE while accounting for  
89 population structure and genotype uncertainty, and evaluate the impact of population  
90 heterogeneity and genotype uncertainty on the standard HWE tests and alternative methods  
91 using simulated and real sequence datasets. Our results demonstrate that ignoring population  
92 structure or genotype uncertainty in HWE tests can inflate false positive rates by many orders  
93 of magnitude. Our evaluations demonstrate different tradeoffs between false positives and  
94 statistical power across the methods, with RUTH consistently amongst the best across all  
95 evaluations. RUTH is implemented as a practical and scalable software tool to rapidly perform  
96 HWE tests across millions of markers and hundreds of thousands of individuals while supporting  
97 standard VCF/BCF formats. RUTH is publicly available at <https://www.github.com/statgen/ruth>.

98

99

## 100 INTRODUCTION

101 Hardy-Weinberg equilibrium (HWE) is a fundamental theorem of population genetics and has  
102 been one of the key mathematical principles to understand the characteristics of genetic  
103 variation in a population for more than a century (HARDY 1908; WEINBERG 1908). HWE describes  
104 a remarkably simple relationship between allele frequencies and genotype frequencies which is  
105 constant across generations in homogeneous, random-mating populations. Genetic variants in  
106 a homogeneous population typically follow HWE except for unusual deviations due to very  
107 strong case-control association and enrichment (NIELSEN *et al.* 1998), sex linkage, or non-  
108 random sampling (WAPLES 2015).

109 HWE tests are often used to assess the quality of microsatellite (VAN OOSTERHOUT *et al.*  
110 2004), SNP-array (WIGGINTON *et al.* 2005), and sequence-based (DANECEK *et al.* 2011) genotypes.  
111 Testing for HWE may reveal technical artifacts in sequence or genotype data, such as high rates  
112 of genotyping error and/or missingness, or sequencing/alignment errors (NIELSEN *et al.* 2011). It  
113 can also identify hemizygotes in structural variants which are incorrectly called as homozygotes  
114 (MCCARROLL *et al.* 2006). Quality control for array-based or sequence-based genotypes typically  
115 includes a HWE test to detect and filter out artifactual or poorly genotyped variants (LAURIE *et*  
116 *al.* 2010; NIELSEN *et al.* 2011).

117 While HWE tests are commonly and reliably used for variant quality control in samples  
118 from homogeneous populations, applying them to more diverse samples remains challenging.  
119 When analyzing individuals from a heterogeneous population, the standard HWE tests may  
120 falsely flag real, well-genotyped variants, unnecessarily filtering them out for downstream  
121 analyses (HAO AND STOREY 2019). This problem is important since genetic studies increasingly

122 collect genetic data from heterogeneous populations. In principle, HWE tests in these  
123 structured populations can be performed on smaller cohorts with homogenous backgrounds  
124 (BYCROFT *et al.* 2018), and the test statistics combined using Fisher's or Stouffer's method  
125 (MOSTELLER AND FISHER 1948; STOUFFER 1949). However, such a procedure requires much more  
126 effort than using a single HWE test across all samples and information that may be imperfect or  
127 unavailable.

128 Here, we describe RUTH (Robust Unified Test for Hardy-Weinberg Equilibrium) which  
129 tests for HWE under heterogeneous population structure. Our primary motivation for  
130 developing RUTH is to robustly filter out artifactual or poorly genotyped variants using HWE  
131 test statistics. RUTH is (1) computationally efficient, (2) robust against various degrees of  
132 population structure, and (3) flexible in accepting key representations of sequence-based  
133 genotypes including best-guess genotypes and genotype likelihoods. We perform systematic  
134 evaluations of RUTH and alternative methods for HWE testing using simulated and real data to  
135 explore the advantages and disadvantages of these methods for samples of diverse ancestries.

## 136 MATERIALS AND METHODS

### 137 Unadjusted HWE tests

138 Consider a study of  $n$  participants with true (unobserved) genotypes  $g_1, g_2, \dots, g_n$  at a bi-allelic  
139 variant coded as 0 (reference homozygote), 1 (heterozygote), or 2 (alternate homozygote).  
140 Represent the best-guess/hard-call (observed) genotypes as  $\hat{g}_1, \hat{g}_2, \dots, \hat{g}_n$ . A simple HWE test  
141 uses the chi-squared statistic to compare the expected and observed genotype counts  
142 assuming no population structure and no genotype uncertainty. The chi-squared HWE test

---

143 statistic is defined as  $T_{\chi^2} = \sum_{k=0}^2 \frac{(c_k - \hat{c}_k)^2}{\hat{c}_k}$  where  $c_j = \sum_{i=0}^n I(\hat{g}_i = j)$  (ignoring missing  
144 genotypes),  $\hat{p} = \frac{c_1 + 2c_2}{2n}$ ,  $\hat{q} = 1 - \hat{p}$ ,  $\hat{c}_0 = n\hat{q}^2$ ,  $\hat{c}_1 = 2n\hat{p}\hat{q}$ , and  $\hat{c}_2 = n\hat{p}^2$ . Under HWE, the  
145 asymptotic distribution of  $T_{\chi^2}$  is usually assumed to follow  $\chi_1^2$  (ROHLFS AND WEIR 2008). An exact  
146 test is known to be more accurate for finite samples, particularly for rare variants (WIGGINTON *et*  
147 *al.* 2005). HWE tests stratified by case-control status are known to prevent an inflation of Type I  
148 errors for disease-associated variants (LI AND LI 2008). Widely used software tools such as PLINK  
149 (PURCELL *et al.* 2007) and VCFTools (DANECEK *et al.* 2011) implement an exact HWE test based on  
150 best-guess genotypes. We will refer to the exact test as the unadjusted test.

## 151 Existing HWE tests accounting for structured populations

152 The unadjusted HWE test assumes that the population is homogeneous. If a study is comprised  
153 of a set of discrete structured subpopulations, a straightforward extension of the unadjusted  
154 test is to (1) stratify each study participant into exactly one of the subpopulations, (2) perform  
155 the unadjusted HWE test for each subpopulation separately, and (3) meta-analyze test statistics  
156 across subpopulations to obtain a combined p-value using Stouffer's method (STOUFFER *et al.*  
157 1949). More specifically, let  $z_1, z_2, \dots, z_s$  be the z-scores from HWE test statistics for  $s$  distinct  
158 subpopulations with sample sizes  $n_1, n_2, \dots, n_s$ . A combined meta-analysis HWE test statistic  
159 across the subpopulations is then  $T_{meta} = \frac{\sum_{i=1}^s z_i \sqrt{n_i}}{\sqrt{\sum_{i=1}^s n_i}}$ , which asymptotically follows a standard  
160 normal distribution when each subpopulation follows HWE.

161 When the population cannot be easily stratified into distinct subpopulations (e.g. intra-  
162 continental diversity or an admixed population), a quantitative representation of genetic

163 ancestry, such as principal component (PC) coordinates or fractional mixture over  
164 subpopulations, can be more useful for representing each study participant's genetic diversity  
165 (ROSENBERG *et al.* 2002; PRICE *et al.* 2006). HWES takes PCs as additional input to perform HWE  
166 tests under population structure with logistic regression (SHA AND ZHANG 2011), and a similar  
167 idea was suggested by Hao and colleagues (2016). However, existing implementations do not  
168 support sequence-based genotypes (where genotype uncertainty may remain at low or  
169 moderate sequencing depth) or other commonly used formats for genetic array data. A recent  
170 method, PCAngsd estimates PCs from uncertain genotypes represented as genotype likelihoods  
171 (MEISNER AND ALBRECHTSEN 2019) and uses these estimates to perform a likelihood ratio test (LRT)  
172 for HWE, which is similar to the LRT version of RUTH with differences in computational  
173 performance (see below).

#### 174 **Robust HWE testing with RUTH**

175 Here we describe RUTH (Robust and Unified Test for Hardy-Weinberg equilibrium) to enable  
176 HWE testing under structured populations, which is especially useful for large sequencing  
177 studies. We developed RUTH to produce HWE test statistics to allow quality control of  
178 sequence-based variant callsets from increasingly diverse samples. RUTH models the  
179 uncertainty encoded in sequence-based genotypes to robustly distinguish true and artifactual  
180 variants in the presence of population structure, and seamlessly scales to millions of individuals  
181 and genetic variants.

182 We assume the observed genotype for individual  $i$  can be represented as a genotype  
183 likelihood (GL)  $L_i^{(G)} = \Pr(Data_i | g_i = G)$ , where  $Data_i$  represents observed data (e.g.  
184 sequence or array), and  $g_i \in \{0,1,2\}$  the true (unobserved) genotype. For example, GLs for

185 sequence-based genotypes can be represented as  $L_i^{(G)} = \prod_{j=1}^{d_i} \Pr(r_{ij}|g_i = G; q_{ij})$  where  $d_i$  is  
186 the sequencing depth,  $r_{ij}$  is the observed read, and  $q_{ij}$  is the corresponding quality score  
187 (EWING AND GREEN 1998; JUN *et al.* 2012). We model GLs for best-guess genotypes  $\hat{g}_i$  from SNP  
188 arrays as  $L_i^{(G)} = (1 - e_i)^2, 2e_i(1 - e_i), e_i^2$  for  $\hat{g}_i = 2, 1, 0$  where  $e_i$  is assumed per-allele error  
189 rate. Imputed genotypes may also be approximately modeled using this framework, but the  
190 current implementation requires creating a pseudo-genotype likelihood to describe this  
191 uncertainty (see Discussion).

## 192 Accounting for Population Structure with Individual-Specific Allele Frequencies

193 We account for population structure by modeling individual-specific allele frequencies from  
194 quantitative coordinates of genetic ancestry such as PCs, similar to the model (HAO *et al.* 2016).  
195 For any given variant, instead of assuming that genotypes follow HWE with a single universal  
196 allele frequency across all individuals, we assume that genotypes follow HWE with  
197 heterogeneous allele frequencies specific to each individual, modeled as a function of genetic  
198 ancestry. Let  $\mathbf{x}_i \in \mathbb{R}^k$  represent the genetic ancestry of individual  $i$ , where  $k$  is the number of  
199 PCs used. We estimate individual-specific allele frequency  $p$  as a bounded linear function of  
200 genetic ancestry

$$201 \quad p(\mathbf{x}_i; \boldsymbol{\beta}) = \begin{cases} \boldsymbol{\beta}^T \mathbf{x}_i & \varepsilon \leq \boldsymbol{\beta}^T \mathbf{x}_i \leq 1 - \varepsilon \\ \varepsilon & \boldsymbol{\beta}^T \mathbf{x}_i < \varepsilon \\ 1 - \varepsilon & \boldsymbol{\beta}^T \mathbf{x}_i > 1 - \varepsilon \end{cases},$$

202 where  $\varepsilon$  is the minimum frequency threshold. We used  $\varepsilon = \frac{1}{4n}$  in our evaluation. Even though  
203 we used a linear model for  $p(\mathbf{x}_i; \boldsymbol{\beta})$  for computational efficiency, it is straightforward to apply a  
204 logistic model, which is arguably better (YANG *et al.* 2012; HAO *et al.* 2016).

205 Let  $p_i = p(x_i; \beta)$  and  $q_i = 1 - p_i$  be the individual specific allele frequencies of the  
206 non-reference and reference alleles for individual  $i$ . Under the null hypothesis of HWE, the  
207 frequencies of genotypes (0, 1, 2) are  $[q_i^2, 2p_iq_i, p_i^2]$ . Under the alternative hypothesis, we  
208 assume these frequencies are  $[q_i^2 + \theta p_iq_i, 2p_iq_i(1 - \theta), p_i^2 + \theta p_iq_i]$  where  $\theta$  is the  
209 inbreeding coefficient. This model is a straightforward extension of a fully general model where  
210  $p_i, q_i$  is identical across all samples. Then the log-likelihood across all study participants is

211 
$$l(\beta, \theta) = \sum_{i=1}^n \log \left[ L_i^{(0)}(q_i^2 + \theta p_iq_i) + L_i^{(1)} 2p_iq_i(1 - \theta) + L_i^{(2)}(p_i^2 + \theta p_iq_i) \right]$$

212 Under both the null ( $\theta = 0$ ) and alternative ( $\theta \neq 0$ ) hypotheses, we maximize the log-  
213 likelihood using an Expectation-Maximization (E-M) algorithm (DEMPSTER *et al.* 1977). As we  
214 empirically observed quick convergence within several iterations in most cases, we used a fixed  
215 ( $n=20$ ) number of iterations in our implementation.

216 **RUTH Score Test**

217 The score function of the log-likelihood is

218 
$$U(\theta) = \sum_{i=1}^n \frac{p_i q_i \left[ L_i^{(0)} - 2L_i^{(1)} + L_i^{(2)} \right]}{L_i^{(0)}(q_i^2 + \theta p_i q_i) + L_i^{(1)} 2p_i q_i(1 - \theta) + L_i^{(2)}(p_i^2 + \theta p_i q_i)} = \sum_{i=1}^n u_i(\theta)$$

219 Since  $u'_i(\theta) = -u_i^2(\theta)$ , we construct a score test statistic of  $H_0: \theta = 0$  vs  $H_1: \theta \neq 0$  as:

220 
$$T_{score} = \frac{[U(0)]^2}{I(0)} = \frac{[\sum_{i=1}^n u_i(0)]^2}{\sum_{i=1}^n u_i^2(0)}$$

221 where  $I(0)$  is the Fisher information under the null hypothesis. Under the null,  $T_{score}$  has an  
222 asymptotic chi-squared distribution with one degree of freedom, i.e.  $T_{score} \sim \chi_1^2$ . We estimate  $\hat{\beta}$   
223 with an E-M algorithm.

224 **RUTH Likelihood Ratio Test**

225 The log-likelihood function  $l(\beta, \theta)$  can also be used to calculate a likelihood ratio test statistic:

226

$$T_{LRT} = 2 \left[ \max_{\beta, \theta} l(\beta, \theta) - \max_{\beta} l(\beta, 0) \right].$$

227 Like the score test, we estimate MLE parameters  $\beta, \theta$  iteratively using an E-M algorithm to test  
228  $H_0: \theta = 0$  vs  $H_1: \theta \neq 0$ . Under the null hypothesis, the asymptotic distribution of  $T_{LRT}$  is  
229 expected to follow  $\chi_1^2$ . This test is very similar to the likelihood-ratio test proposed by PCAngsd  
230 (MEISNER AND ALBRECHTSEN 2019), except PCAngsd does not re-estimate  $\beta$  under the alternative  
231 hypothesis. In principle, the RUTH LRT should be slightly more powerful due to this difference;  
232 we expect the practical difference in power to be small, as deviations from HWE usually do not  
233 change the estimates of  $\beta$  substantially.

234 **Simulation of genotypes and sequence reads under population structure**

235 We simulated sequence-based genotypes under population structure using the following  
236 procedure. First, for each variant, we simulated an ancestral allele frequency and population-  
237 specific allele frequencies. Second, we sampled unobserved (true) genotypes based on these  
238 allele frequencies. Third, we sampled sequence reads based on the unobserved genotypes.  
239 Fourth, we generated genotype likelihoods and best-guess genotypes based on sequence reads.

240 To simulate ancestral and population-specific allele frequencies, we followed the  
241 BALDING AND NICHOLS (1995) procedure, except we sampled ancestral allele frequencies from  
242  $p \sim Uniform(0,1)$  instead of  $p \sim Uniform(0.1, 0.9)$  to include rare variants. For each of  $K \in$   
243  $\{1, 2, 5, 10\}$  populations, we sampled population-specific allele frequencies from  
244  $p_k \sim Beta\left(\frac{p(1-F_{st})}{F_{st}}, \frac{(1-p)(1-F_{st})}{F_{st}}\right)$ , where  $k \in \{1, \dots, K\}$ , and  $F_{st} \in \{.01, .02, .03, .05, .10\}$  was  
245 the fixation index to quantify the differentiation between the populations, as suggested by  
246 Holsinger (HOLSINGER 1999) and implemented in previous studies (HOLSINGER *et al.* 2002; BALDING  
247 2003). Because  $p_k$  no longer follows the uniform distribution, we used rejection sampling to  
248 ensure that  $\bar{p} = \frac{1}{K} \sum_{k=1}^K p_k$  is uniformly distributed across 100 bins across simulations to avoid  
249 artifacts caused by systematic differences in allele frequencies.

250 The unobserved genotype  $G_i \in \{0, 1, 2\}$  for individual  $i \in \{1, \dots, n_k\}$ , belonging to  
251 population  $k$  with sample size  $n_k$ , was simulated from genotype frequencies  $(q_k^2 +$   
252  $\theta p_k q_k, 2p_k q_k(1 - \theta), p_k^2 + \theta p_k q_k)$ , where  $q_k = 1 - p_k$  and  $\theta \in \left[-\min\left(\frac{q_k}{p_k}, \frac{p_k}{q_k}\right), 1\right]$  quantifies  
253 deviation from HWE;  $\theta = 0$  represents HWE, while  $\theta < 0$  and  $\theta > 0$  represent excess  
254 heterozygosity and homozygosity compared to HWE expectation, respectively. In our  
255 experiments, we evaluated  $\theta \in \{0, \pm.01, \pm.05, \pm.1, \pm.5\}$ . When  $\theta$  was smaller than the  
256 minimum possible value for a specific population, we replaced it with the minimum value.

257 We simulated sequence reads based on unobserved genotypes, sequence depths, and  
258 base call error rates. To reflect the variation of sequence depths between individuals, we  
259 simulated the mean depth of each sequenced sample to be distributed as  
260  $\mu_i \sim Uniform(1, 2D - 1)$ , where  $D$  is the expected depth and  $D = 5$  and  $D = 30$  representing  
261 low-coverage and deep sequencing, respectively. For each sequenced sample and variant site,

262 we sampled the sequence depth from  $d_i \sim \text{Poisson}(\mu_i)$ . Each sequence read carried either of  
263 the possible unobserved (true) alleles  $r_{ij} \in \{0,1\}$ , where  $j \in \{1, \dots, d_i\}$ . Given unobserved  
264 genotype  $G_i$ , we generated  $r_{ij} \sim \text{Bernoulli}\left(\frac{G_i}{2}\right)$ , with observed allele  $o_{ij} = (1 - e_{ij})r_{ij} +$   
265  $e_{ij}(1 - r_{ij})$  flipping to the other allele when a sequencing error occurs with probability  
266  $e_{ij} \sim \text{Bernoulli}(\epsilon)$ . We used  $\epsilon = 0.01$  throughout our simulations (which corresponds to phred-  
267 scale base quality of 20) and assumed that all base calling errors switched between reference  
268 and alternate alleles.

269 We then generated genotype likelihoods and best-guess genotypes from the simulated  
270 alleles. Let  $t_i = \sum_{j=1}^{d_i} o_{ij}$  be the observed alternate allele count. The GLs for the three possible  
271 genotypes are  $L_i^{(0)} = (1 - \epsilon)^{d_i - t_i} (\epsilon)^{t_i}$ ,  $L_i^{(1)} = 0.5^{d_i}$ ,  $L_i^{(2)} = (\epsilon)^{d_i - t_i} (1 - \epsilon)^{t_i}$ . We called best-  
272 guess genotypes by using the overall ancestral allele frequency  $\bar{p}$  for a given variant as the  
273 prior, then calling the genotype corresponding to the highest posterior probability among  
274  $(L_i^{(0)}(1 - \bar{p})^2, 2L_i^{(1)}\bar{p}(1 - \bar{p})^2, L_i^{(2)}\bar{p}^2)$  for each sample. For each possible combination of  $F_{st}$ ,  
275  $K$ , and  $\theta$ , we generated 50,000 independent variants across a set of  $n = 5,000$  samples with  
276 per-ancestry samples sizes  $n_k = \frac{n}{K}$ .

## 277 **Evaluation of Type I Error and Statistical Power**

278 We used different p-value thresholds,  $F_{st}$  values, number of ancestry groups  $K$ , and average  
279 sequencing depth  $D$  to determine the number of variants significantly deviating from HWE. To  
280 evaluate Type I error, we simulated sequence reads under HWE ( $\theta = 0$ ) and calculated the  
281 proportion of significant variants at each p-value threshold. In RUTH tests, we assumed PCs  
282 were accurately estimated using true genotypes unless indicated otherwise. For real data, we

283 summarized ancestral information by projecting PCs estimated from their full genomes onto  
284 the reference PC space of the Human Genome Diversity Panel (HGDP) (LI *et al.* 2008) using  
285 verifyBamID2 (ZHANG *et al.* 2020), similar to the procedure for variant calling in the TOPMed  
286 Project, which has already integrated RUTH as part of its quality control pipeline  
287 ([https://github.com/statgen/topmed\\_variant\\_calling](https://github.com/statgen/topmed_variant_calling)).

288 In all datasets, we evaluated the tradeoff between Type I Error and power for each  
289 method using precision-recall curves (PRCs) and receiver-operator characteristic curves (ROCs).  
290 In simulated data, we considered variants with  $\theta = 0$  to be true negatives and variants with  
291  $\theta = -0.05$  to be true positives. In both our 1000G and TOPMed data, we labeled HQ variants as  
292 negative and LQ variants as positive.

### 293 **Data source**

294 To evaluate our method, we used sequence-based genotype data from the 1000 Genomes  
295 Project (1000G) (THE 1000 GENOMES PROJECT CONSORTIUM *et al.* 2015) and the Trans-Omics  
296 Precision Medicine (TOPMed) Project (TALIUN *et al.* 2019). In both cases, we used a subset of  
297 variants from chromosome 20. For 1000G, we started with 1,812,841 variants in 2,504  
298 individuals, with an average depth of 7.0  $\times$ . For TOPMed, we started with 12,983,576 variants  
299 in 53,831 individuals, with an average depth of 37.2  $\times$ .

### 300 **Application to 1000 Genomes data**

301 To test our method on 1000G data, we first needed to define two sets of variants: one set  
302 which is expected to follow HWE, and another set which is expected to deviate from HWE.  
303 Unlike simulated data, variants in 1000G are not clearly classified into “true” or “artifactual”, so

304 evaluation of false positives and power is less straightforward. We focused on two subsets of  
305 variants in chromosome 20 which serve as proxies for these two variant types. We selected  
306 non-monomorphic sites found in both the Illumina Infinium Omni2.5 genotyping array and in  
307 HapMap3 (THE INTERNATIONAL HAPMAP CONSORTIUM *et al.* 2010) as “high-quality” (HQ) variants that  
308 mostly follow HWE after controlling for ancestry, ending up with 17,740 variants. Similarly, we  
309 selected variants that displayed high discordance between duplicates or Mendelian  
310 inconsistencies within family members in TOPMed sequencing study as “low quality” (LQ)  
311 variants that should be enriched for deviations from HWE even after accounting for ancestry,  
312 ending up with 10,966 variants. Among 329,699 LQ variants from TOPMed in chromosome 20,  
313 we found that only 10,966 overlap with 1000 Genome samples because likely artifactual  
314 variants were stringently filtered prior to haplotype phasing. We suspect that a substantial  
315 fraction of these 10,966 LQ variants are true variants since they passed all of the 1000G  
316 Project’s quality filters. Nevertheless, we still expect a much larger fraction of these LQ variants  
317 to deviate from HWE compared to HQ variants.

318 We evaluated multiple representations of sequence-based genotypes from 1000G. As  
319 1000G samples were sequenced at relatively low-coverage of  $7.0 \times$  on average, best-guess  
320 genotypes inferred only from sequence reads (raw GT) tend to have poor accuracy. Therefore,  
321 the officially released best-guess genotypes in 1000G were estimated by combining genotype  
322 likelihoods (GL), calculated based on sequence reads, with haplotype information from nearby  
323 variants through linkage-disequilibrium (LD)-aware genotype refinement using SHAPEIT2  
324 (DELANEAU *et al.* 2013). This procedure resulted in more accurate genotypes (LD-aware GT), but  
325 it implicitly assumed HWE during refinement. As different representations of sequence  
326 genotypes may result in different performance in HWE tests, we evaluated all three different

327 representations - raw GT, LD-aware GT, and GL. In all tests of RUTH using hard genotype calls,  
328 we assumed the error rate for GT-based genotypes to be 0.5%, which is representative of a  
329 typical non-reference genotype error rate for SNP arrays. We restricted our analyses to biallelic  
330 variants. The positions and alleles of 1000G and TOPMed variants were matched using the  
331 liftOver software tool (KUHN *et al.* 2013).

332 We evaluated all tests as described above. For meta-analysis with Stouffer's method, we  
333 divided the samples into 5 strata, using the five 1000G super population code labels – African  
334 (AFR), Admixed American (AMR), East Asian (EAS), European (EUR), and South Asian (SAS). To  
335 obtain PC coordinates for 1000G samples, we estimated 4 PCs from the aligned sequence reads  
336 (BAM) with verifyBamID2 (ZHANG *et al.* 2020), using PCs from 936 samples from the Human  
337 Genome Diversity Project (HGDP) panel as reference coordinates. The RUTH score test and LRT  
338 used these PCs as inputs, along with genotypes in raw GT, LD-aware GT, and GL formats. For  
339 PCAngsd, we used GLs from all variants tested as the input. We limited the analysis to a single  
340 chromosome due to the heavy computational requirements of PCAngsd.

### 341 **Application to TOPMed Data**

342 We analyzed variants from 53,831 individuals from the TOPMed sequencing study (TALIUN *et al.*  
343 2019). These samples came from multiple studies from a diverse spectrum of ancestries,  
344 leading to substantial population structure. Using the same criteria as our 1000G analysis, we  
345 identified 17,524 high-quality variants and 329,699 low-quality variants across chromosome 20.  
346 Since TOPMed genomes were deeply sequenced at  $37.2 \times$  ( $\pm 4.5 \times$ ), LD-aware genotype  
347 refinement was not necessary to obtain accurate genotypes. Therefore, we used two genotype  
348 representations – raw GT and GL – in our evaluations.

349 Similar to 1000G, for best-guess genotypes (raw GT), we used PLINK for the unadjusted  
350 test. For meta-analysis, we assigned each sample to one of the five 1000G super populations as  
351 follows. First, we summarized the genetic ancestries of aligned sequenced genomes with  
352 verifyBamID2 by estimating 4 PCs using HGDP as reference. Second, we used Procrustes  
353 analysis (DRYDEN AND MARDIA 1998; WANG *et al.* 2010) to align the PC coordinates of HGDP panels  
354 (to account for different genome builds) so that the PC coordinates were compatible between  
355 TOPMed and 1000G samples. Third, for each TOPMed sample, we identified the 10 closest  
356 corresponding individuals from 1000G using the first 4 PC coordinates with a weighted voting  
357 system (assigning the closest individual a score of 10, next closest a score of 9, and so on until  
358 the 10th closest individual is assigned a score of 1, then adding up the scores for each super  
359 population) to determine the super population code that had the highest sum of scores, and  
360 therefore best described that sample. In this way, we classified 15,580 samples as AFR, 4,836 as  
361 AMR, 29,943 as EUR, 2,960 as EAS, and 716 as SAS. Among these samples, 94.5% had the same  
362 super population code for all 10 nearest 1000G neighbors. To evaluate the RUTH score test and  
363 LRT for both raw GT and GL, we used 4 PCs estimated by verifyBamID2 (ZHANG *et al.* 2020),  
364 consistent with the method applied for the 1000G data.

### 365 **Impact of Ancestry Estimates on Adjusted HWE Tests**

366 We examined the effect of changing the number of PCs used as input for RUTH tests by using 2  
367 PCs as opposed to 4 PCs. We also evaluated the impact of using different approaches to classify  
368 ancestry when adjusting for population structure with meta-analysis. By default, our analysis  
369 classified the 1000 Genomes subjects into 5 continental super populations based on published  
370 information (THE 1000 GENOMES PROJECT CONSORTIUM *et al.* 2015). For TOPMed, the best-matching

371 1000 Genomes continental ancestry was carefully determined using the PCA-based matching  
372 strategy described above. However, in practice, ancestry classification may be performed with a  
373 coarser resolution (JIN *et al.* 2019). To mimic such a setting, we used k-means clustering on the  
374 first 2 PCs of our samples to divide individuals into 3 distinct groups, and performed meta-  
375 analyses based on this coarse classification for both 1000G and TOPMed data.

376 **Software and data availability**

377 RUTH is available at <https://github.com/statgen/ruth>. Genotype data from 1000G is available  
378 from the International Genome Sample Resource at <https://www.internationalgenome.org>.  
379 TOPMed data is available via a dbGaP application for controlled-access data (see  
380 <https://www.ncbi.nlm.nih.gov/gap> for details).

381 **RESULTS**

382 **Simulation: Effect of Genotype Uncertainty**

383 To evaluate the impact of genotype uncertainty, we first compared tests in the absence of  
384 population structure (i.e. single ancestry). For the unadjusted test, we used only best-guess  
385 genotypes (GTs). For PCAngsd, we used only genotype likelihoods (GLs). For RUTH score and  
386 likelihood ratio tests, we used both.

387 Using GLs over GTs substantially reduced Type I errors in HWE tests, especially in low-  
388 coverage data (Figure 1A-C). For example, the standard HWE test based on GTs resulted in a  
389 229-fold inflation (22.9%) at  $p < .001$  (Figure 1B, Table S1), a threshold which allows the  
390 evaluation of Type I error with reasonable precision with 50,000 variants (50 expected false

391 positives under the null). GT-based RUTH-Score and RUTH-LRT tests showed similar inflation.  
392 When GLs were used instead of best-guess genotypes, RUTH-Score and RUTH-LRT had Type I  
393 errors close to the null expectation (.001 for RUTH-Score and .0012 for RUTH-LRT). PCAngsd,  
394 which also accounts for genotype uncertainty (MEISNER AND ALBRECHTSEN 2019), had similar  
395 performance. The severely inflated Type I errors with best-guess genotypes can largely be  
396 attributed to high uncertainty and bias towards homozygote reference genotypes in single site  
397 calls from low-coverage sequence data, resulting in apparent deviations from HWE. For high-  
398 coverage sequence data, inflation of Type I error with GTs was substantially attenuated;  
399 inflation nearly disappeared when using GLs (.004 for RUTH-Score and .002 for RUTH-LRT;  
400 Figure 1D-F).

401 Next, we evaluated the power to identify variants truly deviating from HWE at various  
402 levels of inbreeding coefficient ( $\theta$ ). For low-coverage sequence data, we skip interpretation of  
403 power of GT-based tests owing to their extremely inflated false positive rates. All GL-based  
404 tests behaved similarly, achieving ~19-21% power at  $p < .001$  with moderate excess  
405 heterozygosity ( $\theta = -0.05$ ) (Figure 2B, Table S1). For high-coverage sequence data, the power of  
406 GL-based tests at the same p-value threshold increased to ~56-60%, comparable to  
407 corresponding GT-based tests. Interestingly, the unadjusted GT-based test showed much lower  
408 power than RUTH and PCAngsd tests under excess heterozygosity ( $\theta < 0$ ) while demonstrating  
409 much higher power with excess homozygosity ( $\theta > 0$ ). Upon further investigation, we observed  
410 that the tests behave very differently for rare variants for which an asymptotic approximation  
411 performs poorly.

412 We also generated precision-recall curves (PRC) and receiver-operator characteristic  
413 (ROC) curves to better understand the tradeoff between the Type I errors and power under  
414 moderate excess heterozygosity ( $\theta = -.05$ ) (Figure S1C-D). Again, accounting for genotype  
415 uncertainty resulted in better empirical power and Type I error, especially for low-coverage  
416 data, for which, at an empirical false positive rate of 1%, GL-based tests had 41-45% power, as  
417 opposed to 4-10% for GT-based tests. For high-coverage data, GL-based tests had 1-2% greater  
418 power than GT-based tests at the same false positive rate. These results suggest that ignoring  
419 genotype uncertainty in HWE tests is reasonable for high-coverage sequence data.

## 420 **Simulation: Impact of Population Structure on HWE Test Statistics**

421 As expected, the unadjusted HWE test had substantially inflated Type I errors under population  
422 structure based on the Balding-Nichols (1995) model (Figure 1, Table S1). Even for an intra-  
423 continental level of population differentiation ( $F_{ST} = .01$ ), the Type I errors at  $p < .001$  were  
424 inflated 13.5-fold even for high-coverage data. With an inter-continental level of differentiation  
425 ( $F_{ST} = .1$ ), we observed orders of magnitude more Type I errors across different simulation  
426 conditions. This inflation is expected to increase with larger sample sizes, suggesting that  
427 adjustment for population structure is important even if a study focuses on a single continental  
428 population.

429 One simple approach to account for population structure is to stratify individuals into  
430 distinct subpopulations to apply HWE tests separately (BYCROFT *et al.* 2018), and meta-analyze  
431 the results (Figure 3B). Type I errors were appropriately controlled with this approach in high-  
432 coverage but not low-coverage data, likely due to unmodeled genotype uncertainty (Figure 1,  
433 Table S1). Instead of classifying individuals into distinct subpopulations, RUTH incorporates PCs

434 to jointly perform HWE tests (Figure 3C). For both low- or high-coverage data, GL-based RUTH  
435 tests and PCAngsd showed well-controlled Type I errors, while GT-based tests showed slight  
436 (high-coverage) or severe (low-coverage) inflation.

437            Although meta-analysis resulted in well-controlled Type I errors for high-coverage data,  
438 it was considerably less powerful than RUTH. For example, with moderate excess  
439 heterozygosity ( $\theta = -.05$ ) across five ancestries ( $F_{ST} = .1$ ), RUTH tests identified 20-27% more  
440 variants as significant at  $p < .001$  (Figure 2, Table S1) compared to meta-analysis. PRCs also  
441 clearly showed better operating characteristics for RUTH and PCAngsd compared to meta-  
442 analysis (Figure S2). For example, at an empirical false positive rate of 1%, RUTH showed much  
443 greater power (66-68%) than meta-analysis (43%), even though the simulation scenario favors  
444 meta-analysis because samples were perfectly classified into distinct subpopulations.

#### 445 **Application to 1000 Genomes WGS data**

446 Next, we evaluated the performance of various HWE tests in low-coverage (~6x) sequence data  
447 from the 1000 Genomes Project. We evaluated three representations of genotypes - (1) raw GT,  
448 (2) LD-aware GT, and (3) GL, as described in Materials and Methods. Among chromosome 20  
449 variants, we selected 17,740 high-quality (HQ) variants that are polymorphic in GWAS arrays,  
450 and 10,966 low-quality (LQ) variants enriched for genotype discordance in duplicates and trios.  
451 Unlike simulation studies, not all LQ variants are necessarily expected to violate HWE, so we  
452 consider the proportion of significant LQ variants as a lower bound on the sensitivity to identify  
453 significant variants. Similarly, not all HQ variants are necessarily expected to follow HWE,  
454 although we expect most to do so, so that the proportion of significant HQ variants serves as an  
455 upper bound for the false positive rate.

456 Consistent with our simulation results, all tests based on raw GTs generated from low-  
457 coverage sequence data had severe inflation of false positives (Figure 4A, Table 1). This was  
458 true even for HQ variants, presumably due to genotyping errors and bias in raw GTs. Standard  
459 HWE tests, which model neither genotype uncertainty nor population structure, showed the  
460 highest inflation of false positives at 44% for  $p < 10^{-6}$ , a threshold commonly used for HWE  
461 testing in large genetic studies (LOCKE *et al.* 2015; FRITSCHE *et al.* 2016). Modeling population  
462 structure substantially reduced inflation, with RUTH tests showing fewer false positives (0.7-  
463 1.0% at  $p < 10^{-6}$ ) than meta-analysis (2.0% at  $p < 10^{-6}$ ). False positives were inflated across all  
464 methods when using raw GTs.

465 Consistent with our simulation studies, GL-based RUTH tests reduced false positives  
466 even further (0.034% at  $p < 10^{-6}$ ). In contrast to our simulations, PCAngsd demonstrated  
467 considerably higher false positives than RUTH (2.1% at  $p < 10^{-6}$ ), likely because PCAngsd  
468 estimates PCs from the input data without the ability to use externally provided PCs (see  
469 Discussion). The sensitivity for detecting significant LQ variants was also consistent with our  
470 simulations (Figure 4B, Table 1). GL-based tests, which showed better control of false positives,  
471 identified 22-25% of LQ variants as significant at  $p < 10^{-6}$ .

472 Strikingly, while using LD-aware GTs reduced false positives with adjusted tests, it was at  
473 the expense of substantially reduced sensitivity to detect LQ variants. The false positive rates of  
474 any adjusted test with LD-aware GTs were uniformly lower than those of any GL- and raw GT-  
475 based tests across all p-value thresholds (Figure 4A). However, sensitivity was also substantially  
476 reduced with LD-aware genotypes (Figure 4B). For example, at  $p < 10^{-6}$ , GL-based RUTH tests  
477 identified 22-23% of LQ variants significant, while using LD-aware GTs halved the proportions.

478 Running meta-analysis with LD-aware GTs reduced sensitivity even further, likely because the  
479 implicit HWE assumption in the LD-aware genotype refinement algorithms may have further  
480 reduced false positives and sensitivity by altering the LD-aware genotypes to conform to HWE.

481 We evaluated PRCs between HQ and LQ variants to further evaluate this tradeoff. The  
482 results clearly demonstrated that HWE tests using LD-aware GTs are substantially less robust  
483 than tests on other genotype representations (Table S2, Figure S3A). For example, for the RUTH  
484 score test, when LD-aware GTs identified 0.1% of HQ variants as significant, 17% of LQ variants  
485 were identified as significant. However, with raw GT and GL, 24~27% were identified as  
486 significant at the same threshold. Even fewer were significant in meta-analysis with LD-aware  
487 GTs (13%). Similar trends were observed across all thresholds, suggesting that using LD-aware  
488 GTs results in substantially poorer operating characteristics than other genotype  
489 representations. As more accurate genotyping in LD-aware genotype refinement is expected to  
490 improve the performance of QC metrics compared to raw GTs, these results are quite striking,  
491 and highlight a potential oversight in using LD-aware genotypes in various QC metrics for  
492 sequence-based genotypes.

### 493 **Application to TOPMed Deep WGS data**

494 We evaluated the various HWE tests on a subset of the Freeze 5 variant calls from the high-  
495 coverage (~37×) whole genome sequence (WGS) data in the TOPMed Project (TALIUN *et al.*  
496 2019). We identified 17,524 HQ variants and 329,699 LQ variants using the same criteria used  
497 for 1000G variants and evaluated raw GTs and GLs. We did not evaluate PCAngsd due to  
498 excessive computational time (see “Computational cost” below).

499 We first evaluated the false positive rates of different HWE tests indirectly by using HQ  
500 variants. With a >20-fold larger sample size than 1000G, we identified more significant HQ  
501 variants, while the false positive rates were still reasonable with adjusted tests. At  $p < 10^{-6}$ , 74%  
502 of HQ variants were significant with unadjusted tests, while the adjusted GL-based tests  
503 identified  $\sim 0.3\%$  at  $p < 10^{-6}$  (Figure 4C-D, Table 2). Adjusted GT-based tests had only slightly  
504 higher levels of false positives at  $p < 10^{-6}$ . However, inflation was more noticeable at less  
505 stringent p-value thresholds suggesting that GL-based tests may be needed for larger sample  
506 sizes.

507 Next, we evaluated the proportions of LQ variants found to be significant by different  
508 tests to indirectly evaluate their statistical power. GT- and GL-based RUTH tests showed similar  
509 power, while meta-analysis showed considerably lower power. For example, at  $p < 10^{-6}$ , meta-  
510 analysis identified 47% of LQ variants as significant, while RUTH tests identified 54-58%. This  
511 pattern was similar across different p-value thresholds (Figure 4C-D) or choices of LQ variants  
512 (Table S3, Figure S4). Our results suggest that GL-based RUTH tests are suitable for testing HWE  
513 for tens of thousands of deeply sequenced genomes with diverse ancestries, but that using raw  
514 GTs will also result in a comparable performance at typically used HWE p-value thresholds (e.g.  
515  $p < 10^{-6}$ ) when performing QC without access to GLs.

516 We used PRCs to evaluate the tradeoff between empirical false positive rates and  
517 power. Consistent with previous results, the GL-based RUTH test showed the best tradeoff  
518 between false positives and power, while the GT-based RUTH test and meta-analysis were  
519 slightly less robust but largely comparable (Figure S3). Notably, when we evaluated the

520 different methods at an empirical false positive rate of 0.1%, RUTH score tests had ~4% higher  
521 power than RUTH LRT for both raw GTs and GLs (Figure S5-6).

## 522 **Impact of ancestry estimation accuracy on HWE tests**

523 So far, our evaluations relied on genetic ancestry estimates carefully determined with  
524 sophisticated methods (see Materials and Methods). However, simpler approaches may be  
525 used instead during the variant QC step, which may affect the performance of adjusted HWE  
526 tests. We evaluated whether the number of PC coordinates affected the performance of RUTH  
527 tests by comparing the performance of RUTH tests when using 2 PCs to using 4 PCs (default).  
528 The results from both simulated and real datasets consistently demonstrated that using 4 PCs  
529 led to substantially reduced Type I errors compared to using 2 PCs at a similar level of power  
530 (Table S2, Table S4, Figure S7). PRCs also clearly showed that using 4 PCs was more robust  
531 against population structure across both simulated and real datasets (Figure S8).

532 We also evaluated whether the classification accuracy of subpopulations affected the  
533 performance of meta-analysis. Instead of assigning 1000 Genomes individuals into five  
534 continental populations, we used the k-means algorithm on those samples' top 2 PCs to classify  
535 them into 3 crude subpopulations (Figure S9). This led to a much higher false positive rate with  
536 virtually no increase in true positives (Figure S10, Table S2). We saw the same pattern in  
537 simulated data (Figure S8, Table S5).

## 538 **Computational cost**

539 We compared the computational costs of RUTH and PCAngsd for simulated and real data. RUTH  
540 has linear time complexity to sample size, while PCAngsd appears to have quadratic time

541 complexity (Tables 3, S6). RUTH also has low memory requirement compared to PCAngsd (for  
542 example, 14 MB vs 2 GB for 1000 Genomes data). Extrapolating our results to the whole  
543 genome scale, analyzing 1000 Genomes (i.e. 80 million variants) is expected to take 120 CPU-  
544 hours for RUTH, and 3,200 CPU-hours for PCAngsd (with >1 TB memory consumption).  
545 Additionally, RUTH can be parallelized into smaller regions in a straightforward manner.

546 **DISCUSSION**

547 RUTH is a unified, flexible, and robust approach to incorporate genetic ancestry and genotype  
548 uncertainty for testing Hardy-Weinberg Equilibrium capable of handling large amounts of  
549 genotype data with structured populations. Sha and Zhang (2011) proposed HWES, an HWE test  
550 for structured populations, to address some of these challenges, but it has not been widely  
551 used due to the lack of an implementation that supports widely used genotype data formats  
552 (e.g. PED, BED, VCF, or BCF) and inability to handle imputed or uncertain genotypes. Hao and  
553 colleagues (2016) proposed sHWE which can only handle best-guess (hard call) genotypes (i.e.  
554 0, 1, or 2 for biallelic variants) and does not account for genotype uncertainty. MEISNER AND  
555 ALBRECHTSEN (2019) proposed PCAngsd to address some of these issues, but it does not support  
556 the standard VCF/BCF formats for sequence-based genotypes, and its current implementation  
557 scales poorly with genome-wide analyses of large samples.

558 Similar to previous studies (SHA AND ZHANG 2011; HAO *et al.* 2016), our proposed  
559 framework uses individual-specific allele frequencies rather than allele frequencies pooled  
560 across all samples to systematically account for population structure in HWE tests. Unlike  
561 previous studies, we model genotype uncertainty in sequence-based genotypes in a likelihood-  
562 based framework. We implemented two RUTH tests – a score test and a likelihood ratio test

563 (LRT) – to test for HWE under population structure for genotypes with uncertainty. While RUTH  
564 LRT is similar to the independently developed PCAngsd, the software implementation of RUTH  
565 is more flexible, scales much better to large studies, and supports the standard VCF format.

566 We provide a comprehensive evaluation of various approaches for testing HWE using  
567 simulated and real data. Our results demonstrated that modeling population stratification is  
568 necessary for HWE tests on heterogenous populations. We showed that accounting for  
569 genotype uncertainty via genotype likelihoods performs substantially better than testing HWE  
570 with best-guess genotypes, especially for low-coverage sequenced genomes. Importantly, we  
571 included the evaluations for an unpublished but commonly used approach – meta-analysis  
572 across stratified subpopulations, cohorts, or batches. Our results demonstrate that meta-  
573 analysis may be effective in reducing false positives, but at the expense of substantially reduced  
574 power compared to RUTH.

575 We observed that the current implementation of PCAngsd does not scale well to large-  
576 scale sequencing data, though in principle it can be implemented more efficiently, because the  
577 underlying HWE test itself is similar to RUTH LRT. PCAngsd requires loading all genotypes into  
578 memory, which is often infeasible for large sequencing studies. For example, loading all of 1000  
579 Genomes will require ~4.8 TB of memory. In our evaluation of 1000G chromosome 20 variants,  
580 the inability of PCAngsd to estimate PCs from the whole genome may have contributed to the  
581 observed difference in results from RUTH compared to our simulation studies.

582 Although our 1000G experiments demonstrated the unexpected result that using raw  
583 GTs had better sensitivity than using LD-aware GTs at the same empirical false positive rates for  
584 low-coverage data, we do not advocate using raw GTs for low-coverage sequence data. First,  
585 the results for raw GTs were still consistently less robust than GL-based RUTH tests. Moreover,

586 it would be tricky to determine an appropriate p-value threshold when the false positives are  
587 severely inflated. Therefore, we strongly advocate using GL-based RUTH tests for robust HWE  
588 tests with low-coverage sequence data. For the now more typical high-coverage sequence data,  
589 GL-based tests are still preferred, but GT-based RUTH tests should be acceptable for cases in  
590 which genotype likelihoods are unavailable.

591 Our experiment compared using 2 vs 4 PCs only because *verifyBamID2* software tool  
592 estimated up to 4 PCs projected onto HGDP panel by default (ZHANG *et al.* 2020). Because our  
593 method focuses on testing HWE during the QC steps in sequence-based variant calls, a curated  
594 version of PCs, estimated from sequenced cohort themselves, may not be readily available at  
595 the time of HWE test. However, it is possible to use a larger number of PCs (e.g. >10 PCs) if  
596 available at the time of HWE test. We expect that a larger number of PCs will account for finer-  
597 grained population structure and may benefit the performance of HWE test, but additional  
598 experiments are needed to quantify the impact of using larger number of PCs.

599 Our results demonstrate that RUTH score and LRT tests perform similarly in simulated  
600 and experimental datasets. Overall, the RUTH-LRT was slightly more powerful than the RUTH-  
601 score test at the expense of slightly greater false positive rates, although this tendency was not  
602 consistent. We observed that the RUTH tests tended to be slightly more powerful in identifying  
603 deviation from HWE in the direction of excess heterozygosity than excess homozygosity when  
604 compared to adjusted meta-analysis. These results might be caused by the difference between  
605 our model-based asymptotic tests compared to the exact test used in meta-analysis.

606 We did not evaluate our methods on imputed genotypes in this manuscript. Because  
607 imputed genotypes implicitly assume HWE, we suspect that HWE tests based on imputed  
608 genotypes may have reduced power compared to directly genotyped variants. It is possible to

609 use approximate genotype likelihoods instead of best-guess genotypes for imputed genotypes,  
610 but this requires genotype probabilities, not just the genotype dosages. If genotype  
611 probabilities  $\Pr(g_i = G | Data_i)$  are available, they can be converted to genotype likelihoods  
612  $L_i^{(G)} = \Pr(Data_i | g_i = G)$  using Bayes' rule by modeling  $\Pr(g_i = G)$  as a binomial distribution  
613 based on allele frequencies (which implicitly assumes HWE). However, similar to LD-aware  
614 genotypes in low-coverage sequencing, the power of HWE tests with imputed genotypes may  
615 be poor. Further evaluation is needed to understand how useful this approximation will be  
616 compared to alternative methods including the use of best-guess imputed genotypes.

617 Our methods have room for further improvement. First, we used a truncated linear  
618 model for individual-specific allele frequencies for computational efficiency. Although such an  
619 approximation was demonstrated to be effective in practice (ZHANG *et al.* 2020), applying a  
620 logistic model or some other more sophisticated model may be more effective in improving the  
621 precision and recall of RUTH tests. Second, we did not attempt to model or evaluate the effect  
622 of admixture in our method. Because HWE is reached in two generations with random mating,  
623 accounting for admixed individuals may only have marginal impact. On the other hand,  
624 admixture can lead to higher observed heterozygosity. It may be possible to improve RUTH by  
625 explicitly modeling and adjusting for the effect of admixture on individual-specific allele  
626 frequencies. Systematic evaluations focusing on admixed populations are needed to evaluate  
627 RUTH's performance on such samples, and whether an admixture adjustment is necessary.  
628 Third, RUTH tests do not account for family structure. We suspect that the apparent inflation of  
629 Type I error for the TOPMed data was partially due to sample relatedness. Accounting for  
630 family structure in other ways, for example using variance components models, will require  
631 much longer computational times and may not be feasible for large-scale datasets. Fourth,

632 RUTH currently does not directly support imputed genotypes or genotype dosages. In principle,  
633 it is possible to convert posterior probabilities for imputed genotypes into genotype likelihoods  
634 to account for genotype uncertainty (by using individual-specific allele frequencies). However,  
635 because most genotype imputation methods implicitly assume HWE, we suspect that HWE tests  
636 on imputed genotypes will be underpowered, similar to our observations with LD-aware  
637 genotypes in the 1000 Genomes dataset, even though explicitly modeling posterior  
638 probabilities may slightly mitigate this reduction in power.

639 In summary, we have developed and implemented robust and rapid methods and  
640 software tools to enable HWE tests that account for population structure and genotype  
641 uncertainty. We performed comprehensive evaluations of both our methods and alternative  
642 approaches. Our tools can be used to evaluate variant quality in very large-scale genetic data  
643 sets, with the ability to handle standard VCF formats for storing sequence-based genotypes.  
644 Our software tools are publicly available at <http://github.com/statgen/ruth>.

645

---

## 646 Acknowledgements

647 This work was supported by NIH grants HL137182 (from NHLBI), HG009976 (from NHGRI), HG007022  
648 (from NHGRI), DA037904 (from NIDA), HL117626-05-S2 (from NHLBI), and MH105653 (from NIMH).  
649 Molecular data for the Trans-Omics in Precision Medicine (TOPMed) program was supported by the  
650 National Heart, Lung and Blood Institute (NHLBI). Core support including centralized genomic read  
651 mapping and genotype calling, along with variant quality metrics and filtering were provided by the  
652 TOPMed Informatics Research Center (3R01HL-117626-02S1; contract HHSN268201800002I). Core  
653 support including phenotype harmonization, data management, sample-identity QC, and general

654 program coordination were provided by the TOPMed Data Coordinating Center (R01HL-120393; U01HL-  
655 120393; contract HHSN268201800001I). We gratefully acknowledge the studies and participants who  
656 provided biological samples and data for TOPMed.

657 TOPMed source studies and sample counts are described in Table S7. Acknowledgements for TOPMed  
658 omics support are detailed in Table S8. Full TOPMed study acknowledgements are listed in  
659 Supplementary File S1.

660

---

661

662 REFERENCES

663 Balding, D. J., 2003 Likelihood-based inference for genetic correlation coefficients. *Theor Popul Biol* 63: 221-230.

665 Balding, D. J., and R. A. Nichols, 1995 A Method for Quantifying Differentiation between Populations at 666 Multi-Allelic Loci and Its Implications for Investigating Identity and Paternity. *Genetica* 96: 3-12.

667 Bycroft, C., C. Freeman, D. Petkova, G. Band, L. T. Elliott *et al.*, 2018 The UK Biobank resource with deep 668 phenotyping and genomic data. *Nature* 562: 203-209.

669 Danecek, P., A. Auton, G. Abecasis, C. A. Albers, E. Banks *et al.*, 2011 The variant call format and 670 VCFtools. *Bioinformatics* 27: 2156-2158.

671 Delaneau, O., J. F. Zagury and J. Marchini, 2013 Improved whole-chromosome phasing for disease and 672 population genetic studies. *Nat Methods* 10: 5-6.

673 Dempster, A. P., N. M. Laird and D. B. Rubin, 1977 Maximum Likelihood from Incomplete Data Via the 674 EM Algorithm. *Journal of the Royal Statistical Society: Series B (Methodological)* 39: 1-22.

675 Dryden, I. L., and K. V. Mardia, 1998 *Statistical shape analysis*. John Wiley & Sons, Chichester ; New York.

676 Ewing, B., and P. Green, 1998 Base-calling of automated sequencer traces using phred. II. Error 677 probabilities. *Genome Res* 8: 186-194.

678 Fritsche, L. G., W. Igl, J. N. Bailey, F. Grassmann, S. Sengupta *et al.*, 2016 A large genome-wide 679 association study of age-related macular degeneration highlights contributions of rare and 680 common variants. *Nat Genet* 48: 134-143.

681 Hao, W., M. Song and J. D. Storey, 2016 Probabilistic models of genetic variation in structured 682 populations applied to global human studies. *Bioinformatics* 32: 713-721.

683 Hao, W., and J. D. Storey, 2019 Extending Tests of Hardy-Weinberg Equilibrium to Structured 684 Populations. *Genetics* 213: 759-770.

685 Hardy, G. H., 1908 Mendelian Proportions in a Mixed Population. *Science* 28: 49-50.

686 Holsinger, K. E., 1999 Analysis of Genetic Diversity in Geographically Structured Populations: A Bayesian 687 Perspective. *Hereditas* 130: 245-255.

688 Holsinger, K. E., P. O. Lewis and D. K. Dey, 2002 A Bayesian approach to inferring population structure 689 from dominant markers. *Mol Ecol* 11: 1157-1164.

690 Jin, Y., A. A. Schaffer, M. Feolo, J. B. Holmes and B. L. Kattman, 2019 GRAF-pop: A Fast Distance-Based 691 Method To Infer Subject Ancestry from Multiple Genotype Datasets Without Principal 692 Components Analysis. *G3 (Bethesda)* 9: 2447-2461.

693 Jun, G., M. Flickinger, K. N. Hetrick, J. M. Romm, K. F. Doheny *et al.*, 2012 Detecting and estimating 694 contamination of human DNA samples in sequencing and array-based genotype data. *Am J Hum 695 Genet* 91: 839-848.

696 Kuhn, R. M., D. Haussler and W. J. Kent, 2013 The UCSC genome browser and associated tools. *Brief 697 Bioinform* 14: 144-161.

698 Laurie, C. C., K. F. Doheny, D. B. Mirel, E. W. Pugh, L. J. Bierut *et al.*, 2010 Quality control and quality  
699 assurance in genotypic data for genome-wide association studies. *Genet Epidemiol* 34: 591-602.

700 Li, J. Z., D. M. Absher, H. Tang, A. M. Southwick, A. M. Casto *et al.*, 2008 Worldwide human relationships  
701 inferred from genome-wide patterns of variation. *Science* 319: 1100-1104.

702 Li, M., and C. Li, 2008 Assessing departure from Hardy-Weinberg equilibrium in the presence of disease  
703 association. *Genet Epidemiol* 32: 589-599.

704 Locke, A. E., B. Kahali, S. I. Berndt, A. E. Justice, T. H. Pers *et al.*, 2015 Genetic studies of body mass index  
705 yield new insights for obesity biology. *Nature* 518: 197-206.

706 McCarroll, S. A., T. N. Hadnott, G. H. Perry, P. C. Sabeti, M. C. Zody *et al.*, 2006 Common deletion  
707 polymorphisms in the human genome. *Nat Genet* 38: 86-92.

708 Meisner, J., and A. Albrechtsen, 2019 Testing for Hardy-Weinberg Equilibrium in Structured Populations  
709 using Genotype or Low-Depth NGS Data. *Mol Ecol Resour*.

710 Mosteller, F., and R. A. Fisher, 1948 Questions and Answers. *The American Statistician* 2: 30-31.

711 Nielsen, D. M., M. G. Ehm and B. S. Weir, 1998 Detecting marker-disease association by testing for  
712 Hardy-Weinberg disequilibrium at a marker locus. *Am J Hum Genet* 63: 1531-1540.

713 Nielsen, R., J. S. Paul, A. Albrechtsen and Y. S. Song, 2011 Genotype and SNP calling from next-  
714 generation sequencing data. *Nat Rev Genet* 12: 443-451.

715 Price, A. L., N. J. Patterson, R. M. Plenge, M. E. Weinblatt, N. A. Shadick *et al.*, 2006 Principal components  
716 analysis corrects for stratification in genome-wide association studies. *Nat Genet* 38: 904-909.

717 Purcell, S., B. Neale, K. Todd-Brown, L. Thomas, M. A. Ferreira *et al.*, 2007 PLINK: a tool set for whole-  
718 genome association and population-based linkage analyses. *Am J Hum Genet* 81: 559-575.

719 Rohlfs, R. V., and B. S. Weir, 2008 Distributions of Hardy-Weinberg equilibrium test statistics. *Genetics*  
720 180: 1609-1616.

721 Rosenberg, N. A., J. K. Pritchard, J. L. Weber, H. M. Cann, K. K. Kidd *et al.*, 2002 Genetic structure of  
722 human populations. *Science* 298: 2381-2385.

723 Sha, Q., and S. Zhang, 2011 A test of Hardy-Weinberg equilibrium in structured populations. *Genet  
724 Epidemiol* 35: 671-678.

725 Stouffer, S. A., 1949 *The American soldier*. Princeton University Press, Princeton,.

726 Stouffer, S. A., E. A. Suchman, L. C. DeVinney, S. A. Star and R. M. Williams Jr, 1949 The American soldier:  
727 Adjustment during army life.(Studies in social psychology in World War II), Vol. 1.

728 Taliun, D., D. N. Harris, M. D. Kessler, J. Carlson, Z. A. Szpiech *et al.*, 2019 Sequencing of 53,831 diverse  
729 genomes from the NHLBI TOPMed Program. *bioRxiv*.

730 The 1000 Genomes Project Consortium, A. Auton, L. D. Brooks, R. M. Durbin, E. P. Garrison *et al.*, 2015 A  
731 global reference for human genetic variation. *Nature* 526: 68-74.

732 The International HapMap Consortium, D. M. Altshuler, R. A. Gibbs, L. Peltonen, D. M. Altshuler *et al.*,  
733 2010 Integrating common and rare genetic variation in diverse human populations. *Nature* 467:  
734 52-58.

735 Van Oosterhout, C., W. F. Hutchinson, D. P. M. Wills and P. Shipley, 2004 MICRO-CHECKER: software for  
736 identifying and correcting genotyping errors in microsatellite data. *Molecular Ecology Notes* 4:  
737 535-538.

738 Wang, C., Z. A. Szpiech, J. H. Degnan, M. Jakobsson, T. J. Pemberton *et al.*, 2010 Comparing spatial maps  
739 of human population-genetic variation using Procrustes analysis. *Stat Appl Genet Mol Biol* 9:  
740 Article 13.

741 Waples, R. S., 2015 Testing for Hardy-Weinberg proportions: have we lost the plot? *J Hered* 106: 1-19.

742 Weinberg, W., 1908 Über den nachweis der vererbung beim menschen. *Jh. Ver. vaterl. Naturk.*  
743 Wurttemb. 64: 369-382.

744 Wigginton, J. E., D. J. Cutler and G. R. Abecasis, 2005 A note on exact tests of Hardy-Weinberg  
745 equilibrium. *Am J Hum Genet* 76: 887-893.

746 Yang, W. Y., J. Novembre, E. Eskin and E. Halperin, 2012 A model-based approach for analysis of spatial  
747 structure in genetic data. *Nat Genet* 44: 725-731.

748 Zhang, F., M. Flickinger, S. A. G. Taliun, P. P. G. C. In, G. R. Abecasis *et al.*, 2020 Ancestry-agnostic  
749 estimation of DNA sample contamination from sequence reads. *Genome Res* 30: 185-194.

750

751

## 752 **List of Figures and Tables**

753 Figure 1: Evaluation of Type I Errors between various HWE tests on simulated genotypes.

754 Figure 2. Power Evaluation of power between different HWE tests on simulated genotypes.

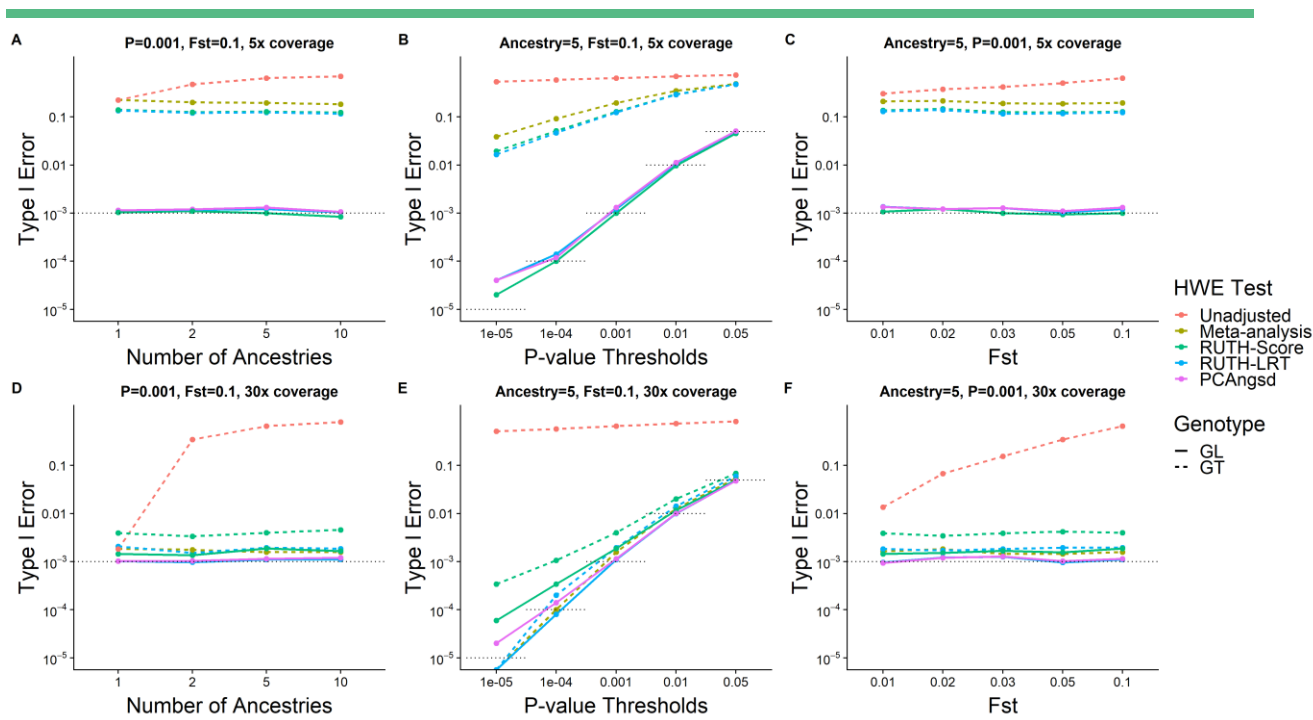
755 Figure 3: Schematic diagrams of different methods to test HWE under population structure.

756 Figure 4. Evaluation of different HWE tests on 1000 Genomes and TOPMed variants.

757 Table 1. Performance of the unadjusted test, meta-analysis, RUTH, and PCAngsd on 1000 Genomes  
758 chromosome 20 variants.

759 Table 2. Performance of the unadjusted test, meta-analysis, and RUTH on TOPMed freeze 5  
760 chromosome 20 variants.

761 Table 3. Runtimes for RUTH and PCAngsd on simulated data.

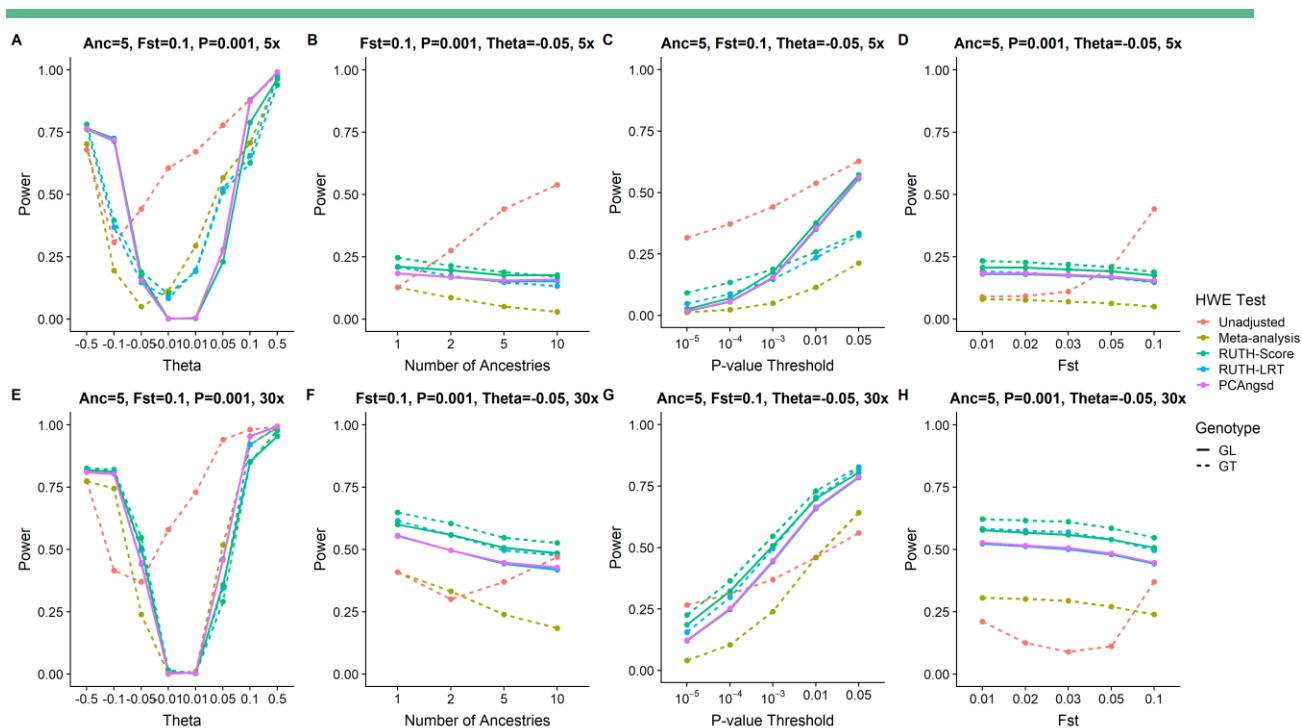


762

763

### Figure 1

764 Evaluation of Type I Errors between various HWE tests on simulated genotypes. Under each combination of  
765 simulation conditions (number of ancestries, sequencing coverage, and fixation index), we simulated 5,000  
766 samples with 50,000 variants that follow HWE within each of the subpopulations and determined the Type I error  
767 performances of different HWE tests based on the proportion of variants labeled as having significant p-values.  
768 Five HWE tests – (1) Unadjusted HWE test (WIGGINTON *et al.* 2005) implemented in PLINK-1.9 (PURCELL *et al.* 2007)  
769 using hard genotypes, (2) meta-analysis using Stouffer's method across ancestries using hard genotypes (GT), (3)  
770 RUTH test using hard genotypes, (4) RUTH test using phred-scale likelihood (GL) computed from simulated  
771 sequence reads, and (5) PCAngsd (MEISNER AND ALBRECHTSEN 2019) – were tested under HWE with various parameter  
772 settings. Gray dotted lines indicate targeted Type I Error rates. Top panels (A-C) represent results from shallow  
773 sequencing (5x), and the bottom panels (D-F) represent results from deep sequencing (30x). Using GL-based  
774 genotypes resulted in Type I Error rates closer to the targeted rate than using GT-based genotypes across different  
775 numbers of ancestries (A, D), P-value thresholds (B, E), and fixation indices (C, F). The difference is especially large  
776 for low-coverage genotypes.

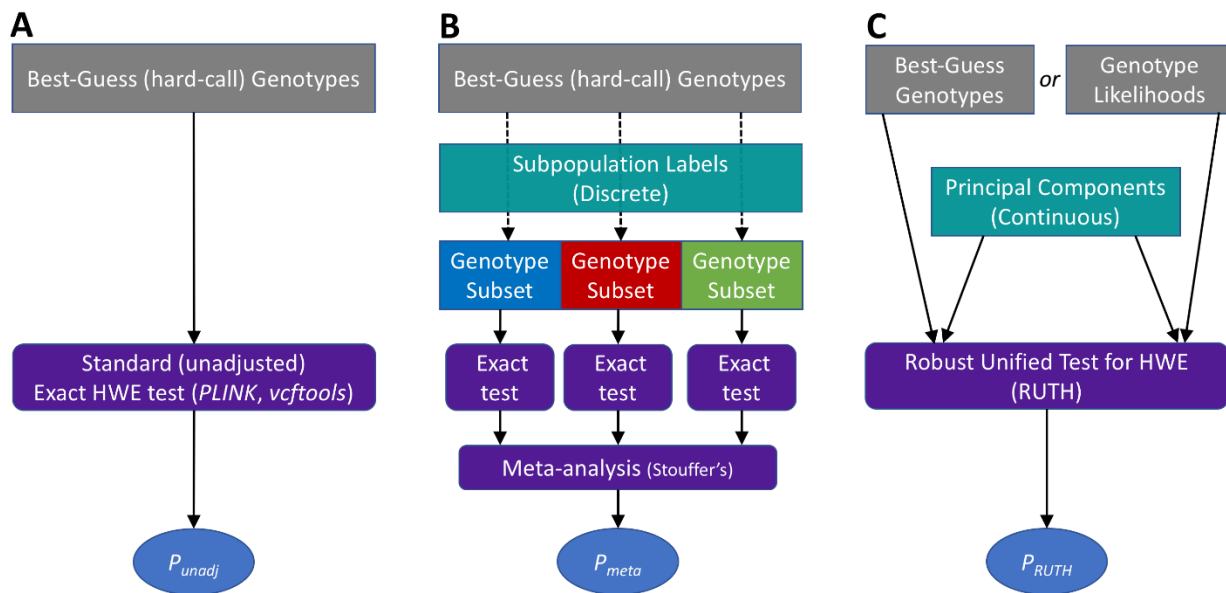


777

778

## Figure 2

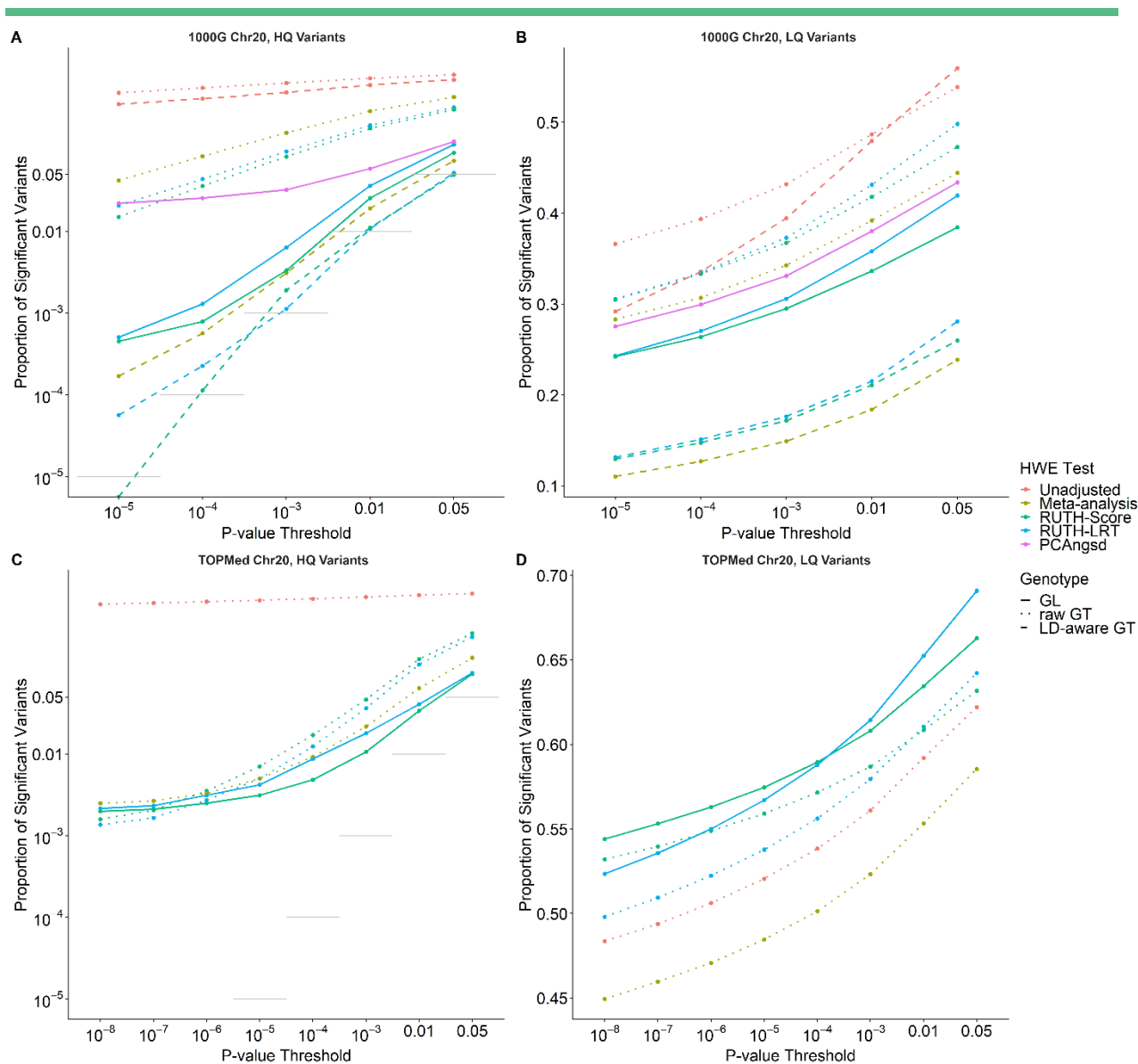
779 Evaluation of power between different HWE tests on simulated genotypes. Under each combination of simulation  
 780 conditions (number of ancestries, sequencing coverage, fixation index, and deviation from HWE), we simulated  
 781 50,000 variants for 5,000 samples and evaluated the ability of different HWE tests to find the variants significant.  
 782 Unless otherwise specified, the default simulation parameters are 5 ancestries, with  $F_{ST}=1$ ,  $P$ -value threshold=.001,  
 783 and  $\Theta=-0.05$ . Tests that can find a larger proportion of significant variants are considered more powerful. Five  
 784 HWE tests – (1) Unadjusted HWE test (WIGGINTON *et al.* 2005) implemented in PLINK-1.9 using hard genotypes (2)  
 785 RUTH test using hard genotypes, (3) RUTH test using phred-scale likelihood (PL) computed from simulated  
 786 sequence reads, (4) meta-analysis using Stouffer's method across ancestries using hard genotypes, and (5)  
 787 PCAngsd (MEISNER AND ALBRECHTSEN 2019) – were tested for variants deviating from HWE with various parameter  
 788 settings, for low coverage (A-D) and high coverage (E-H) data. (A, E) Theta controls the degree of deviation from  
 789 HWE, with negative values indicating excess heterozygosity and positive values indicating heterozygote depletion.  
 790 The high Type I Error rates in GT-based tests (Figure 2) lead to those methods appearing to have higher power in  
 791 some scenarios. The unadjusted test suffers from this problem the most. GL-based methods have slightly lower  
 792 powers than GT-based methods in exchange for a much better controlled Type I error rate. This pattern mostly  
 793 holds across different numbers of ancestries (B, F), p-value thresholds (C, G), and fixation indices (D, H). Meta-  
 794 analysis had the lowest power in the presence of excess heterozygosity.  
 795



796

797 **Figure 3**

798 Schematic diagrams of different methods to test HWE under population structure. Three different methods to test  
799 HWE under population structure are described. (A) In the standard (unadjusted) HWE test, all samples are tested  
800 together using best-guess genotypes. This test does not adjust for sample ancestry. (B) In a meta-analysis of  
801 stratified HWE tests, the samples must first be categorized into discrete subpopulations, determined a priori based  
802 on their genotypes or self-reported ancestries. Next, standard HWE tests (based on best-guess genotypes) are  
803 performed on each of these subpopulations. Then, the resulting HWE statistics are converted into Z-scores and  
804 combined in a meta-analysis using Stouffer's method, with the sample sizes of the subpopulations as weights. (C)  
805 In our proposed method (RUTH), either best-guess genotypes or genotype likelihoods can be used as input for  
806 HWE test. We assume that the genetic ancestries of each sample are estimated a priori, typically as principal  
807 components (PCs). We combine the genotypes and PCs to perform either a score test or a likelihood ratio test to  
808 obtain a joint ancestry-adjusted HWE statistic for each variant across all samples.  
809



810

811

**Figure 4**  
812 Evaluation of different HWE tests on 1000 Genomes and TOPMed variants. In 1000 Genomes data (A, B), we  
813 identified 17,740 “high quality” (HQ) variants and 10,966 “low quality” (LQ) variants in chromosome 20. In  
814 TOPMed data (C, D), we identified 17,524 HQ variants and 329,699 LQ variants in chromosome 20. A well-behaved  
815 HWE test should maximize the proportion of significant LQ variants while controlling the false positive rate for HQ  
816 variants. Dotted gray lines represent targeted Type I error levels if we assume all HQ variants follow HWE. (A) Both  
817 the unadjusted test and PCAngsd found substantially more significant variants than expected in the 1000G HQ  
818 variant set, while both RUTH and meta-analysis were more conservative. Methods that used raw GTs showed  
819 substantial false positive rates, while methods that used GLs and LD-aware GTs had much better control of false  
820 positives. (B) In 1000G LQ variants, meta-analysis lagged behind RUTH and the unadjusted test in discovering  
821 significant deviation from HWE. RUTH behaved well for HQ variants while having more power to find low-quality  
822 variants significantly deviating from HWE. (C) In TOPMed data, the unadjusted test resulted in an excess of false  
823 positives. Tests using GL-based genotypes outperformed tests using GT-based genotypes. (D) Methods using GL-  
824 based genotypes were able to discover more LQ variants than methods using GT-based genotypes, demonstrating  
825 the advantage of accounting for genotype uncertainty in HWE tests.

826

827 **Table 1**

828 Performance of the unadjusted test, meta-analysis, RUTH, and PCAngsd on 1000 Genomes chromosome 20  
 829 variants.

Variant Category	Genotype Format	HWE Test	Proportion of Significant Variants					Total Variant Count
			P < 10 <sup>-2</sup>	P < 10 <sup>-3</sup>	P < 10 <sup>-4</sup>	P < 10 <sup>-5</sup>	P < 10 <sup>-6</sup>	
LQ Variants	raw GT	Unadjusted	0.487	0.432	0.394	0.366	0.339	10,966
		Meta-analysis	0.392	0.343	0.307	0.283	0.262	10,966
		RUTH-Score	0.418	0.367	0.333	0.305	0.284	10,966
		RUTH-LRT	0.431	0.373	0.335	0.305	0.280	10,966
LQ Variants	LD-aware GT	Unadjusted	0.479	0.395	0.336	0.292	0.259	10,966
		Meta-analysis	0.184	0.149	0.127	0.111	0.098	10,966
		RUTH-Score	0.211	0.172	0.147	0.130	0.112	10,966
		RUTH-LRT	0.215	0.177	0.151	0.131	0.115	10,966
HQ Variants	GL	RUTH-Score	0.336	0.295	0.264	0.242	0.223	10,966
		RUTH-LRT	0.358	0.306	0.270	0.243	0.225	10,966
		PCAngsd	0.380	0.331	0.300	0.275	0.255	10,920
		Unadjusted	0.755	0.657	0.573	0.501	0.443	17,740
HQ Variants	raw GT	Meta-analysis	0.298	0.161	0.084	0.042	0.020	17,740
		RUTH-Score	0.183	0.083	0.036	0.015	7.4x10 <sup>-3</sup>	17,740
		RUTH-LRT	0.200	0.095	0.044	0.021	0.010	17,740
		Unadjusted	0.623	0.507	0.422	0.361	0.311	17,740
HQ Variants	LD-aware GT	Meta-analysis	0.019	3.1x10 <sup>-3</sup>	5.6x10 <sup>-4</sup>	1.7x10 <sup>-4</sup>	1.1x10 <sup>-4</sup>	17,740
		RUTH-Score	0.011	1.9x10 <sup>-3</sup>	1.1x10 <sup>-4</sup>	0	0	17,740
		RUTH-LRT	0.011	1.1x10 <sup>-3</sup>	2.3x10 <sup>-4</sup>	5.6x10 <sup>-5</sup>	0	17,740
		RUTH-Score	0.026	3.3x10 <sup>-3</sup>	7.9x10 <sup>-4</sup>	4.5x10 <sup>-4</sup>	3.4x10 <sup>-4</sup>	17,740
	GL	RUTH-LRT	0.036	6.4x10 <sup>-3</sup>	1.3x10 <sup>-3</sup>	5.1x10 <sup>-4</sup>	3.4x10 <sup>-4</sup>	17,740
		PCAngsd	0.059	0.032	0.026	0.022	0.021	17,740

830 The numbers within cells represent the proportions of significant variants under the corresponding testing  
 831 conditions at the given P-value threshold. We expect our LQ variants to violate HWE at a higher rate than our HQ  
 832 variants. A well-behaved test is expected to find a high proportion of LQ variants to be significant while  
 833 maintaining the targeted Type I Error rate in HQ variants. The unadjusted test consistently shows the highest false  
 834 positive rate among all the tests. HWE tests that rely on raw GTs also show much higher false positive rates than  
 835 tests that use other genotype representations. RUTH tests were the best at controlling false positives while still  
 836 maintaining comparable power to the other methods. PCAngsd had a much higher false positive rate than RUTH-  
 837 based methods, especially at more stringent p-value thresholds.  
 838

839 **Table 2**

840 Performance of the unadjusted test, meta-analysis, and RUTH on TOPMed freeze 5 chromosome 20 variants.

841

Variant set	Genotype Format	HWE Test	Proportion of Significant Variants					Total Variant Count
			P < 10 <sup>-2</sup>	P < 10 <sup>-3</sup>	P < 10 <sup>-4</sup>	P < 10 <sup>-5</sup>	P < 10 <sup>-6</sup>	
LQ Variants	raw GT	Unadjusted	0.592	0.561	0.539	0.521	0.506	329,699
	raw GT	Meta-analysis	0.554	0.524	0.502	0.485	0.471	329,699
	raw GT	RUTH-Score	0.608	0.587	0.572	0.559	0.549	329,699
	GL	RUTH-Score	0.635	0.608	0.590	0.575	0.563	329,699
	raw GT	RUTH-LRT	0.610	0.580	0.556	0.538	0.522	329,699
	GL	RUTH-LRT	0.653	0.615	0.588	0.567	0.550	329,699
HQ Variants	raw GT	Unadjusted	0.890	0.842	0.800	0.766	0.736	17,524
	raw GT	Meta-analysis	0.065	0.022	9.0x10 <sup>-3</sup>	4.8x10 <sup>-3</sup>	3.3x10 <sup>-3</sup>	17,524
	raw GT	RUTH-Score	0.145	0.047	0.172	7.1x10 <sup>-3</sup>	3.5x10 <sup>-3</sup>	17,524
	GL	RUTH-Score	0.034	0.011	4.9x10 <sup>-3</sup>	3.1x10 <sup>-3</sup>	2.5x10 <sup>-3</sup>	17,524
	raw GT	RUTH-LRT	0.125	0.036	0.012	5.0x10 <sup>-3</sup>	2.7x10 <sup>-3</sup>	17,524
	GL	RUTH-LRT	0.041	0.018	8.5x10 <sup>-3</sup>	4.3x10 <sup>-3</sup>	3.1x10 <sup>-3</sup>	17,524

842  
843  
844  
845  
846  
847  
848  
849  
850  
851

The numbers within cells represent the proportions of significant variants under the corresponding testing conditions at the given P-value threshold. These results are based on tests that used likelihood-based genotype representations as input. A well-behaved test should reduce the number of significant high-quality (HQ) variants while increasing the number of significant low-quality (LQ) variants. The unadjusted test had a greatly inflated false positive rate for HQ variants while showing a lower true positive rate for LQ variants. While meta-analysis performed better for HQ variants, it had reduced power to find LQ variants to be significant. RUTH performed the best, with fewer false positives (significant HQ variants) compared to both the unadjusted test and meta-analysis, while at the same time finding more true positives (significant LQ variants).

852 **Table 3**

853 Runtimes for RUTH and PCAngsd on simulated data.

Sample Size	Wall Time (s)			User Time (s)		
	RUTH-LRT	RUTH-Score	PCAngsd	RUTH-LRT	RUTH-Score	PCAngsd
1,000	16.21	27.24	173.11	16.16	27.09	172.37
2,000	32.19	54.63	347.10	31.94	54.51	345.58
5,000	82.80	136.44	1,124.83	81.81	136.20	1,102.85
10,000	165.48	273.67	7,396.00	163.88	273.27	7,235.91
20,000	336.75	553.92	38,807.67	332.06	553.05	37,338.69
50,000	902.81	1,438.32	461,971.33	886.67	1,435.87	403,296.5

854

855 We simulated 10,000 genotype likelihood-based variants for varying numbers of samples. Wall time indicates total  
856 runtime, while user time is the amount of time the CPUs spent running each program. All programs were run in  
857 single-threaded mode. System processes make up the difference between the two values, with a majority  
858 consisting of file I/O. We used VCF files with GL fields in RUTH and converted them to Beagle3 format for PCAngsd.  
859 The RUTH likelihood ratio test (LRT) was the fastest method, with the score test about 60% slower. PCAngsd was  
860 about 10 times slower than RUTH-LRT with the smallest sample sizes and over 400 times slower with our largest  
861 tested size of 50,000 samples.  
862

## 863 List of Supplementary Figures, Tables, and File

864 Figure S1. ROC and PRC for simulated single-ancestry data.

865 Figure S2. Precision-recall curves for simulated data with multiple ancestries.

866 Figure S3. Precision-recall curves for 1000G and TOPMed variants.

867 Figure S4. Results of testing TOPMed variants found in 1000G variant list.

868 Figure S5. ROC curves for TOPMed variants found in 1000G variant list.

869 Figure S6. PRC curves for TOPMed variants found in 1000G variant list.

870 Figure S7. Results of testing 1000G and TOPMed variants with RUTH using two vs. four PCs.

871 Figure S8. Effect of ancestry estimation accuracy on Precision-Recall Curves

872 Figure S9. Principal component plots and group assignments for 1000 Genomes and TOPMed samples.

873 Figure S10. Results of testing 1000G and TOPMed variants with meta-analysis using K-means to generate  
874 ancestry groups.

875

876 Table S1. Simulation results for the unadjusted test, meta-analysis, RUTH, and PCAngsd for HWE.

877 Table S2. Results from using lower quality ancestry estimations on meta-analysis and RUTH.

878 Table S3. Performance of the unadjusted test, meta-analysis, and RUTH on the subset of TOPMed freeze  
879 5 chromosome 20 variants that are also found in 1000G.

880 Table S4. Simulation results for RUTH tests using 2 vs 4 principal components.

881 Table S5. The effect of high vs. low quality subpopulation classification on meta-analysis in simulated  
882 samples.

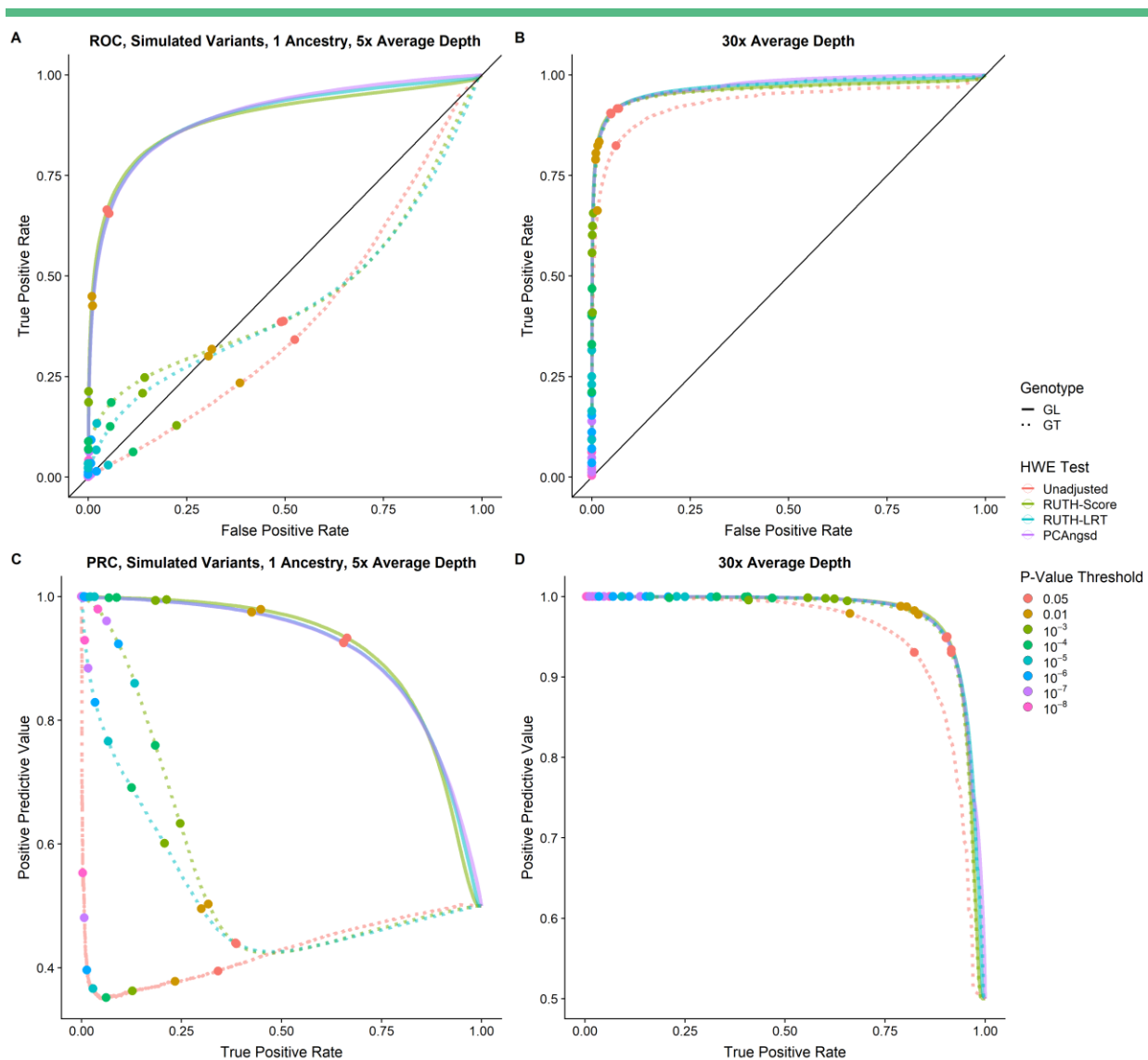
883 Table S6. Comparison of runtimes and memory requirements for RUTH and PCAngsd in simulated and  
884 1000G data.

885 Table S7. Sample contributions from each of the participating TOPMed studies.

886 Table S8. TOPMed acknowledgements for omics support.

887 File S1. TOPMed Study Acknowledgments

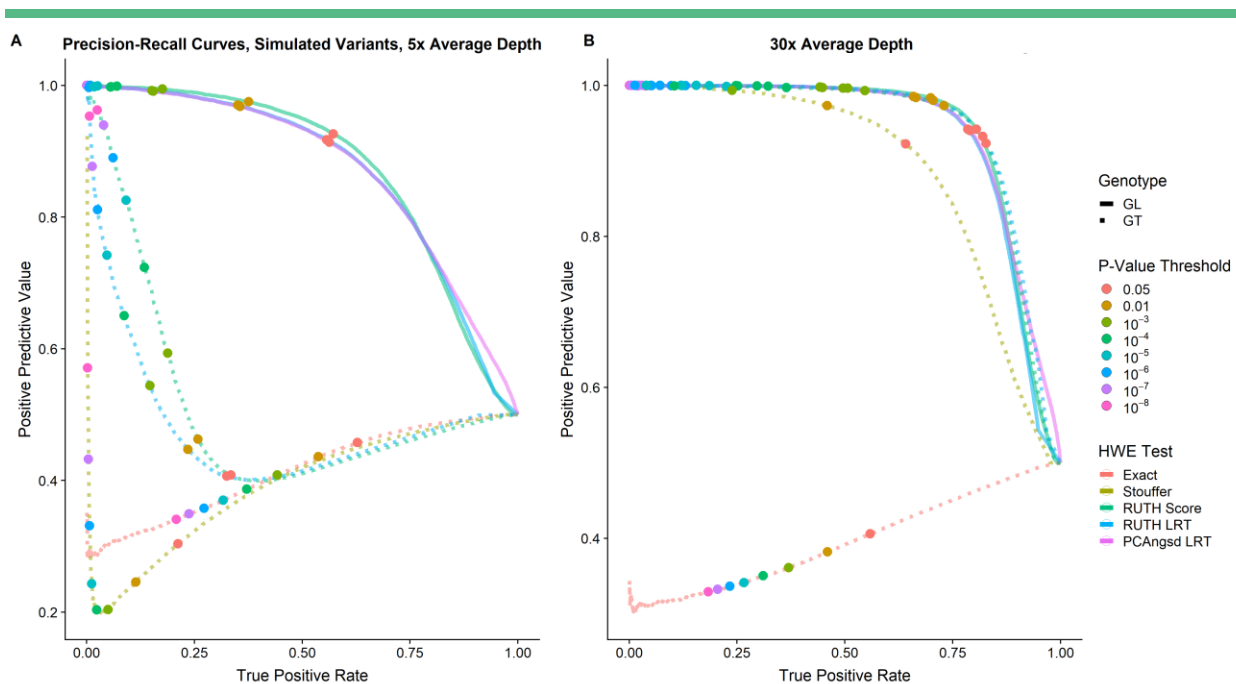
888



889

890 **Figure S1**  
891 ROC and PRC for simulated single-ancestry data. For both low coverage (A, C) and high coverage (B, D) settings,  
892 500,000 variants were generated from 5,000 samples arising from a single ancestry, with half of the variants as  
893 true positives ( $\theta = -0.05$ ) and half of the variants as true negatives ( $\theta = 0$ ). The colors of the lines correspond to the  
894 different HWE tests, while the colors of the points correspond to different P-value thresholds. In all cases, the  
895 unadjusted test performed the worst. For low-coverage data, tests using GT-based genotypes performed poorly  
896 due to their inability to capture the effects of genotype uncertainty, whereas tests using GL-based genotypes  
897 performed much better. The difference was negligible in high-coverage genotype data.

898

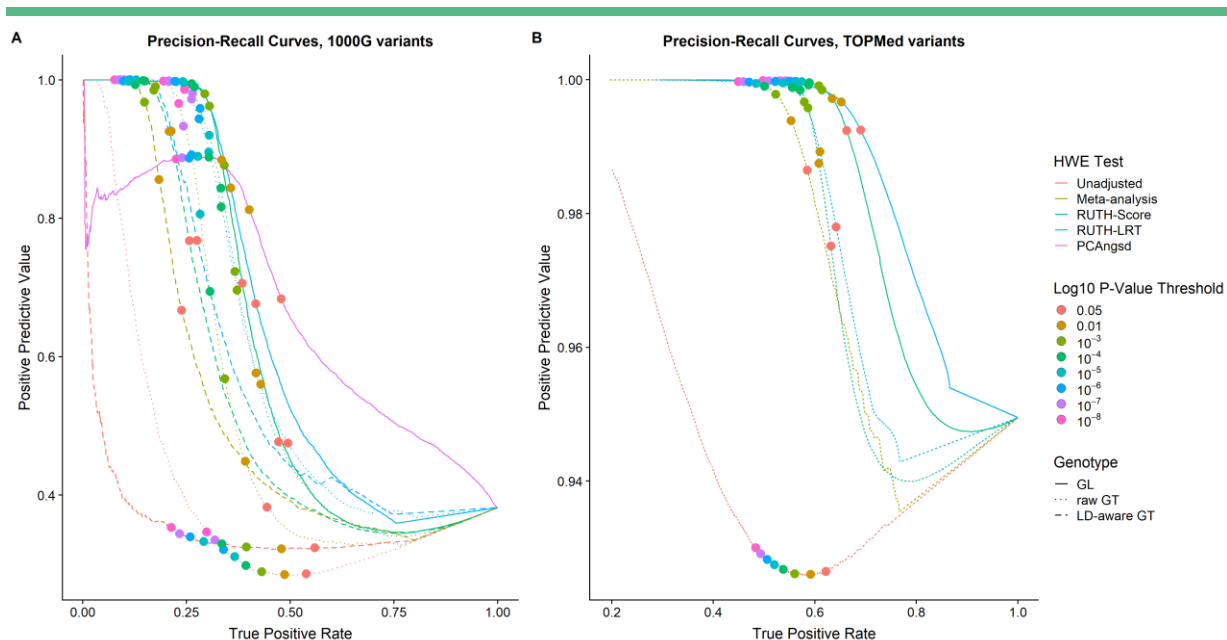


899

900 **Figure S2**

901 Precision-recall curves for simulated data with multiple ancestries. We generated Precision-recall curves to  
902 evaluate the tradeoff between the different HWE tests' ability to identify true positive variants while minimizing  
903 the misidentification of true negative variants as significantly departing from HWE. We analyzed 50,000 true  
904 positive and 50,000 true negative variants in 5,000 samples arising from 5 different ancestries with an average  
905 simulated depth of (A) 5x and (B) 30x. True negative variants are defined as variants with the HWE deviation  
906 parameter  $\theta = 0$ . True positives are defined as variants with  $\theta = -0.05$ . The True Positive Rate (TPR) is defined to be  
907 the proportion of variants with  $\theta = -0.05$  that are significant at a given P-value threshold, while the Positive  
908 Predictive Value (PPV) is defined as the proportion of significant variants with  $\theta = -0.05$  at the same P-value  
909 threshold. Selected p-value thresholds are indicated with colored circles. For low-depth genotypes, in the presence  
910 of high genotype uncertainty, GL-based HWE tests performed relatively well, while GT-based tests performed  
911 poorly. For high-depth genotypes, with low genotype uncertainty, all methods adjusting for population structure  
912 performed relatively well.

913

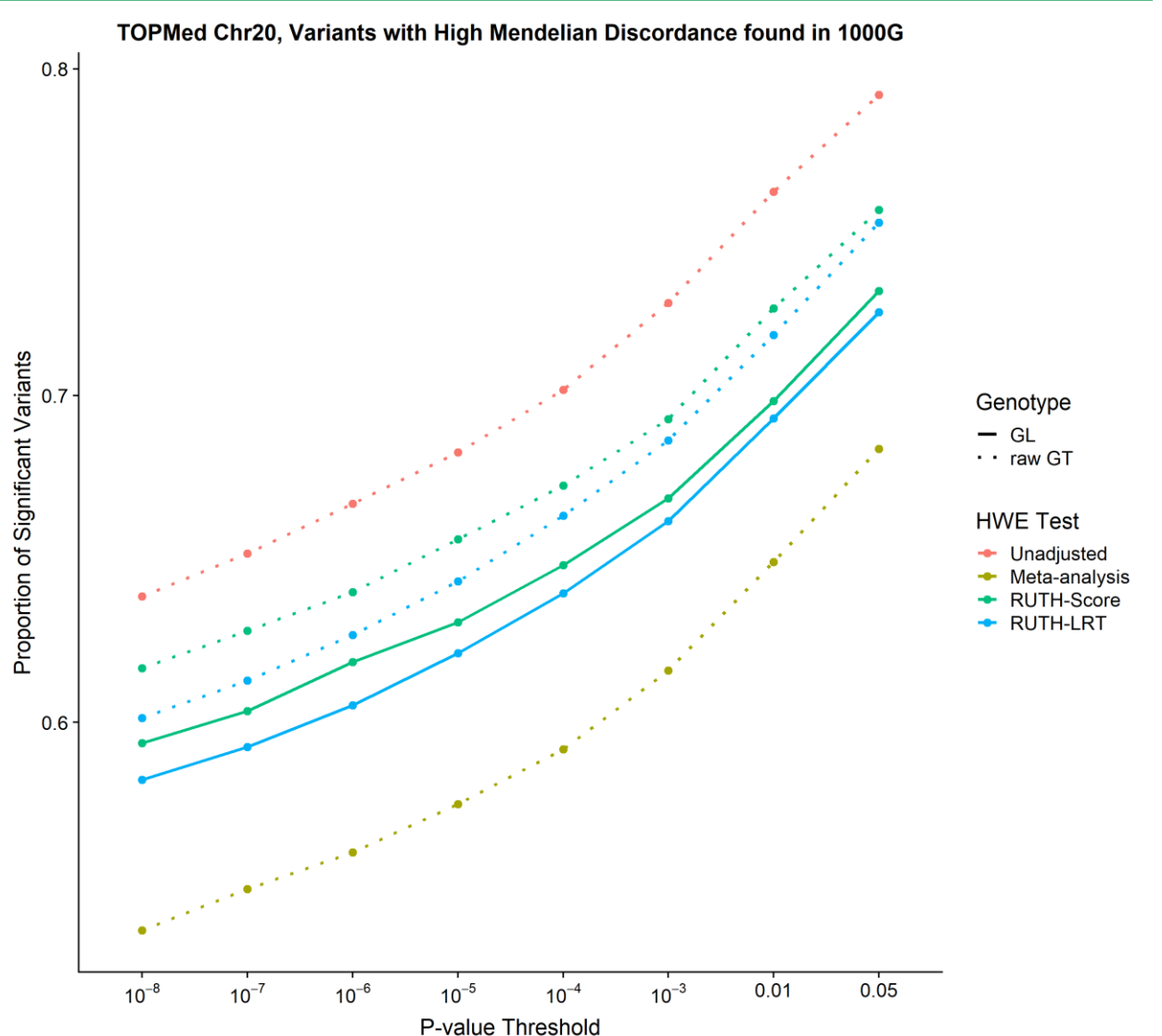


914

915 **Figure S3**

916 Precision-recall curves for 1000G and TOPMed variants. We defined positive variants as those with a high level of  
917 Mendelian inconsistency in family-based TOPMed data, and negative variants as those found in the intersection of  
918 the Illumina Omni2.5 and HapMap3 variant site lists. (A) For low-coverage sequence data found in 1000G, tests  
919 using GL-based genotypes (solid lines) generally performed better than tests using any GT-based genotypes  
920 (dotted and dashed lines). Both the unadjusted test and meta-analysis performed much worse than all other  
921 methods. (B) For high-coverage sequence data found in TOPMed, tests using GL-based genotypes retained their  
922 improved performance over tests using GT-based genotypes.

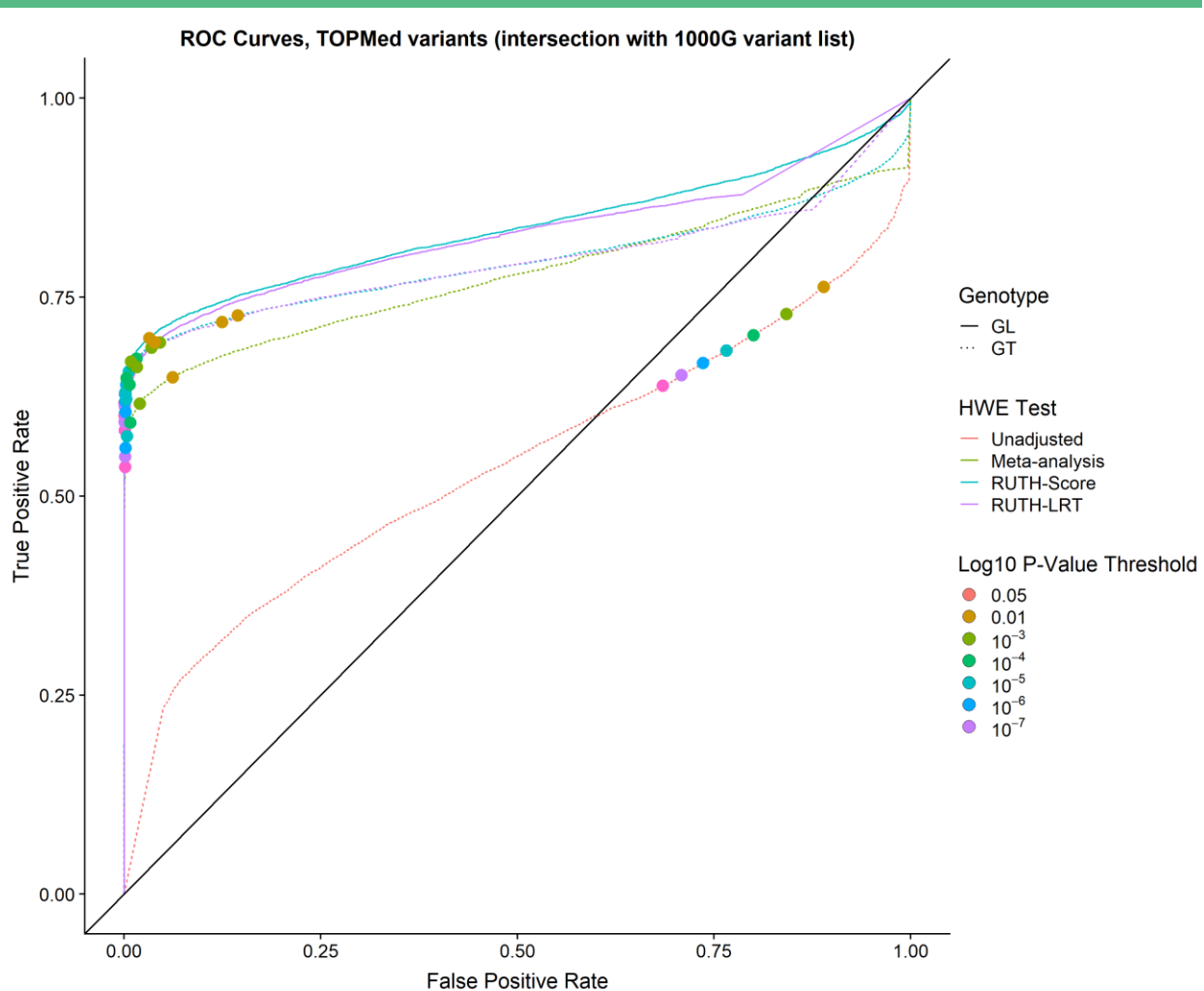
923



924

925 **Figure S4**

926 Results of testing TOPMed variants found in 1000G variant list. This analysis contains 10,966 TOPMed variants  
927 found to be discordant in TOPMed family data and overlapping with 1000G discordant variants, as opposed to all  
928 329,699 discordant TOPMed variants (as seen in Figure 4D). Our results are similar to those for 1000G discordant  
929 variants (Figure 4B), suggesting that the differences between the patterns observed in 1000G and TOPMed results  
930 may have been caused by the difference in allele frequency distributions in the two data sets (Table S1).  
931

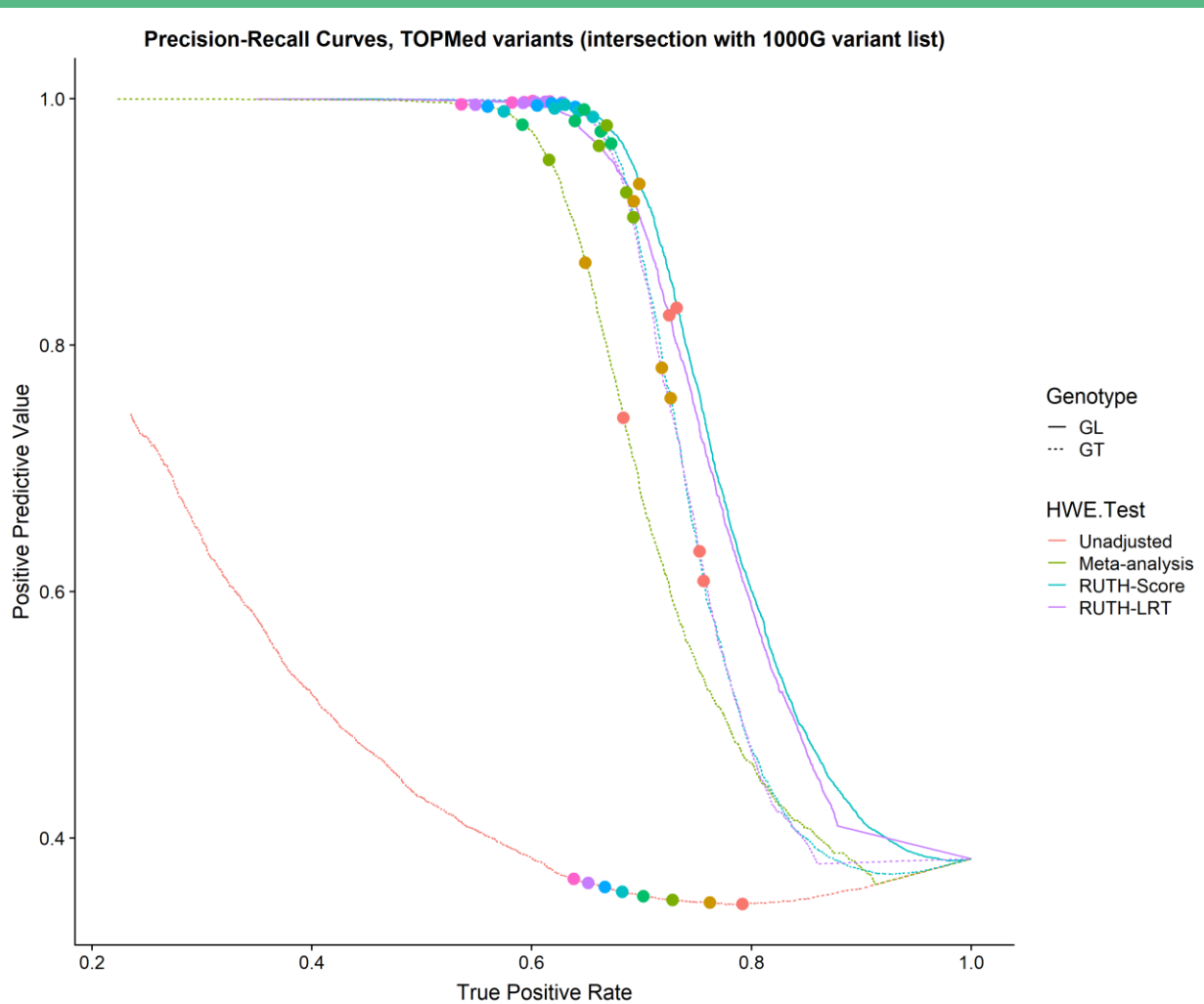


932

933 **Figure S5**

934 ROC curves for TOPMed variants found in 1000G variant list. GL-based tests have the best overall performance  
935 among the different methods.

936

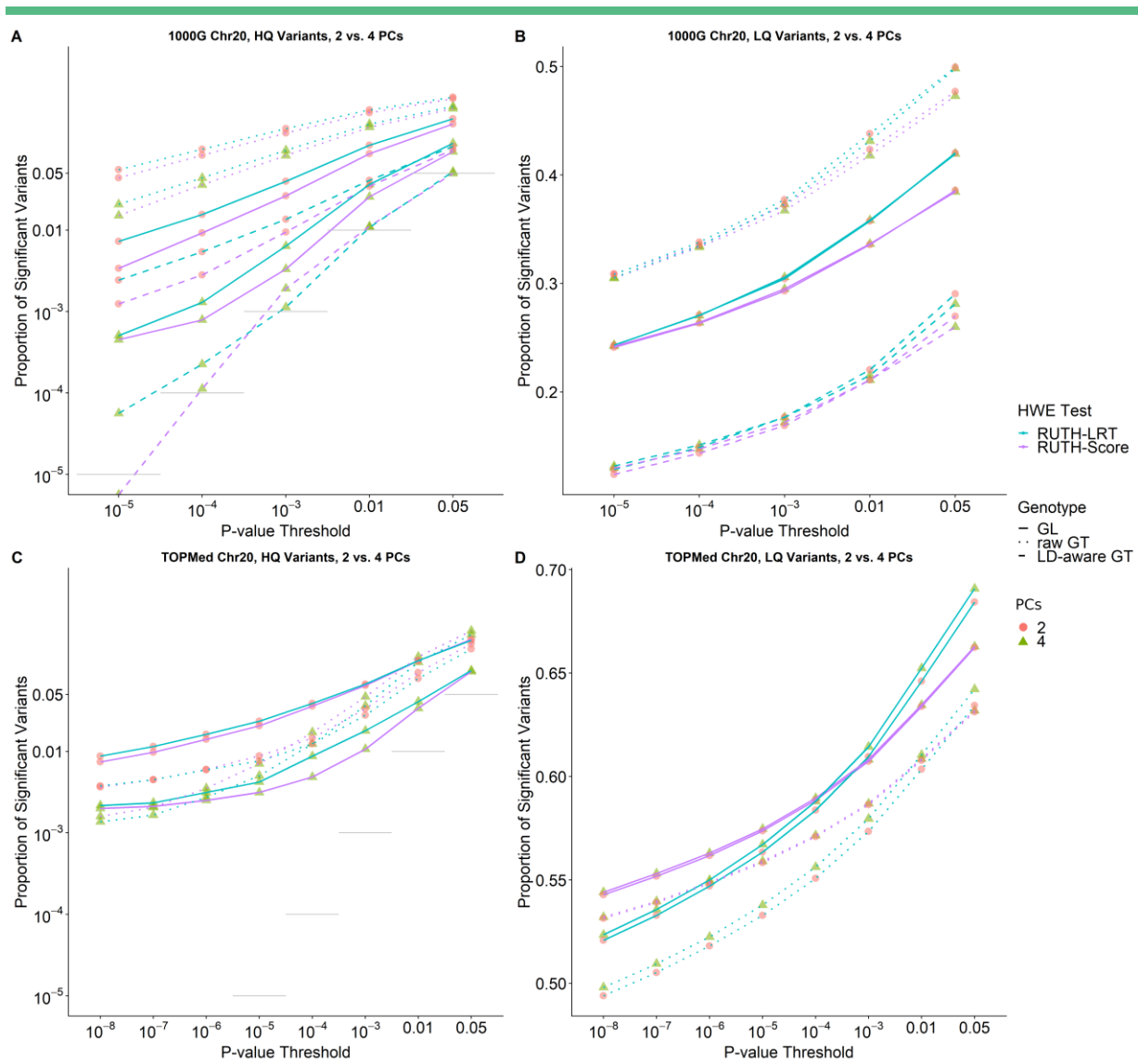


937

938 **Figure S6**

939 PRC curves for TOPMed variants found in 1000G variant list. RUTH tests using GLs offer the best balance between  
940 finding true positives and maximizing positive predictive value.

941

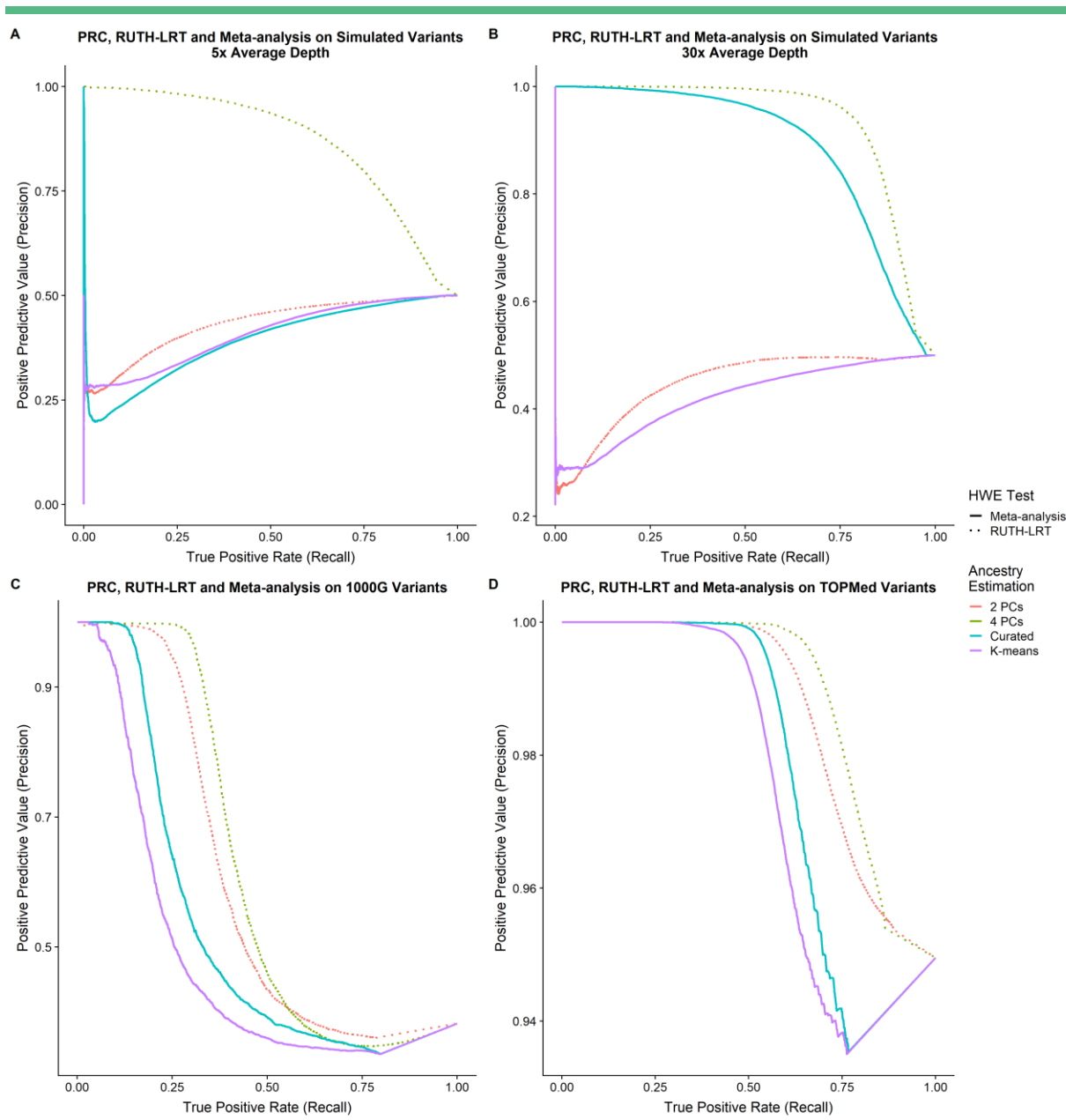


942

943 **Figure S7**

944 Results of testing 1000G and TOPMed variants with RUTH using two vs. four PCs. Using only 2 PCs lead to  
 945 noticeably worse performance, especially for GL-based tests. (A) In 1000 Genomes data, using only 2 PCs leads to  
 946 much higher false positives in HQ variants for both RUTH-Score and RUTH-LRT compared to using 4 PCs. (B) Tests  
 947 on LQ variants with 2 PCs appear to have modestly higher power than tests using 4 PCs, but this is mainly due to  
 948 the much higher false positive rate. (C) For HQ variants in TOPMed, tests using only 2 PCs have substantially higher  
 949 false positive rate than tests using 4 PCs for GL-based tests, while GT-based tests are comparable. (D) Surprisingly,  
 950 GL-based tests using 4 PCs discovered more significant LQ variants compared to GL-based tests using 2 PCs, even  
 951 though GL-based tests using 2 PCs had a higher false positive rate in HQ variants.

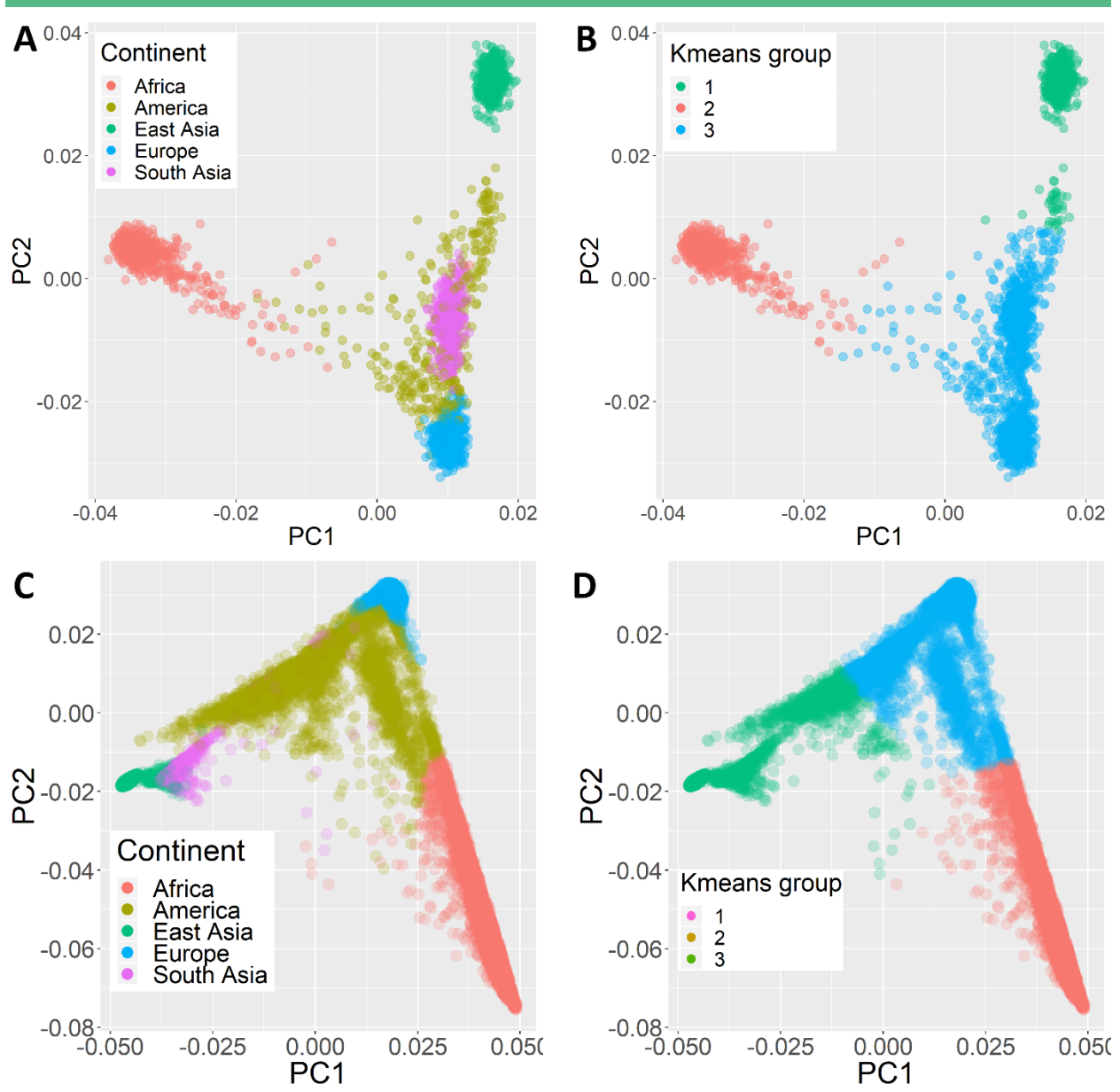
952



953

954 **Figure S8**

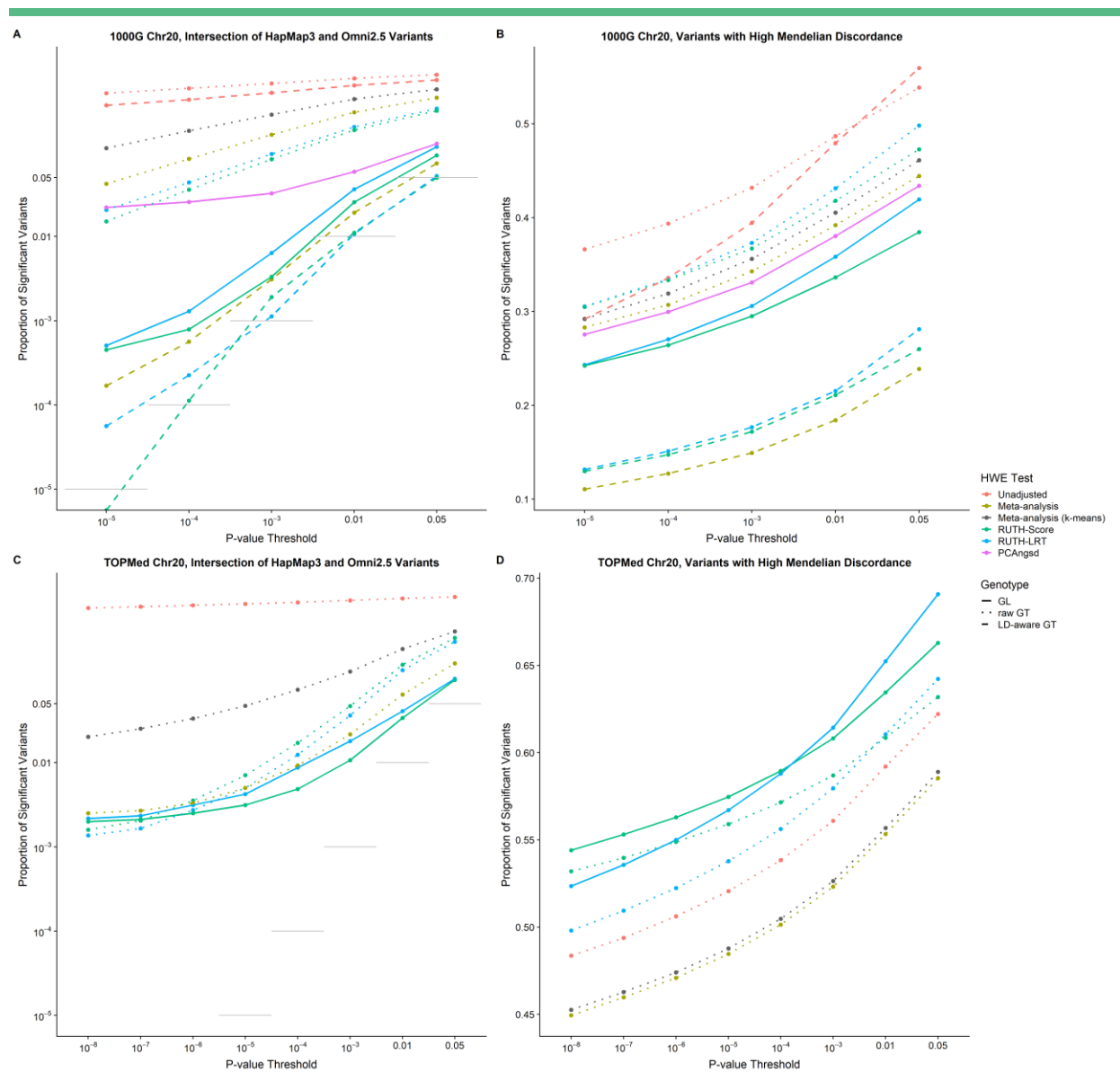
955 Effect of ancestry estimation accuracy on Precision-Recall Curves. We evaluated the effect of using 2 vs. 4 principal  
 956 components on the performance of RUTH-LRT, and the effect of using our nearest-neighbor algorithm (“curated”)  
 957 vs. k-means for subpopulation classification of samples on the performance of meta-analysis on (A) low-depth  
 958 simulated data, (B) high-depth simulated data, (C) 1000G variants, and (D) TOPMed variants. We simulated null  
 959 variants with  $\theta = 0$  and alternative variants with  $\theta = -0.05$ , with a fixation index of 0.1 for 5,000 samples from 5  
 960 ancestries (1,000 samples each). RUTH-LRT used GL-based genotypes, and meta-analysis used raw GT-based  
 961 genotypes. K-means classification for simulated data was performed assuming 3 subpopulation clusters.  
 962



963

964 **Figure S9**

965 Principal component plots and group assignments for 1000 Genomes and TOPMed samples. Ancestry group  
966 assignments for samples in 1000G (A, B) and TOPMed (C, D) samples used either a high-quality ancestry estimation  
967 method (A, C) or a crude k-means based method (B, D). In meta-analysis, samples within a group were first  
968 analyzed together using the unadjusted test. Then, the group-level results were combined using Stouffer's method.  
969 Meta-analyses using the cruder k-means groupings performed much worse than those using the high-quality  
970 ancestry estimates due to population stratification within the cruder groups.  
971



972

973 **Figure S10**

974 Results of testing 1000G and TOPMed variants with meta-analysis using K-means to generate ancestry groups. We  
 975 generated three subpopulations for 1000G and TOPMed separately by applying k-means to the first two principal  
 976 components of each group. Next, we calculated subpopulation-specific HWE statistics, which were converted to Z-  
 977 scores and combined using Stouffer's method, using each subpopulation's size as the weights. (A) K-means-based  
 978 meta-analysis had much higher false positive rates in 1000G compared to meta-analysis that used more accurate  
 979 population labels, which (B) confounds its seemingly higher power to discover true positives. (C) We see the same  
 980 increased false positive rate in K-means-based meta-analysis in TOPMed, but surprisingly (D) it also reduced the  
 981 power to discover true positives in TOPMed. High-quality ancestry groups can substantially improve the  
 982 performance of ancestry-based meta-analysis.

983

---

984 **Table S1**

985 Simulation results for the unadjusted test, meta-analysis, RUTH, and PCAngsd for HWE.

986 This table can be found at the following link:

987 [https://docs.google.com/spreadsheets/d/1zdn7jOWgOMG\\_wwqwgDD4b1i0a2clGlyNFKml5xR\\_DoE/edit?usp=sharing](https://docs.google.com/spreadsheets/d/1zdn7jOWgOMG_wwqwgDD4b1i0a2clGlyNFKml5xR_DoE/edit?usp=sharing)

988 Results from various HWE tests for simulations with 50,000 variants for 5,000 samples. Samples were generated  
989 using a population fixation index ( $F_{ST}$ ) between .01 and .1. “GL” indicates a method using genotype likelihoods,  
990 while “GT” indicates a method using best-guess genotypes. Theta denotes deviation from HWE: Theta = 0 indicates  
991 no deviation from HWE, Theta < 0 indicates excess heterozygosity, and Theta > 0 indicates heterozygote depletion.  
992 When the samples were generated from a single ancestry, meta-analysis and the unadjusted test were identical.

993 \*Combined  $F_{ST}$  indicates the combined results for  $F_{ST}=.01, .02, .03, .05$ , and .1. This is available only when the  
994 number of ancestries is 1, because  $F_{ST}$  should not affect the results with single ancestry, so the results may be  
995 combined.

996  
997

998 **Table S2**

999 Results from using lower quality ancestry estimations on meta-analysis and RUTH.

Data set	Variant set	Genotype Format	HWE Test	PCs	Proportion of Significant Variants					Total Variant Count
					P < 0.01	P < 10 <sup>-3</sup>	P < 10 <sup>-4</sup>	P < 10 <sup>-5</sup>	P < 10 <sup>-6</sup>	
1000G	LQ	raw GT	Meta-analysis	n/a	0.392	0.343	0.307	0.283	0.262	10,966
			Meta-analysis (k-means)	n/a	0.405	0.356	0.319	0.292	0.269	10,966
		LD-aware GT	Meta-analysis	n/a	0.184	0.149	0.127	0.111	0.098	10,966
			Meta-analysis (k-means)	n/a	0.221	0.169	0.136	0.116	0.102	10,966
	HQ	raw GT	Meta-analysis	n/a	0.298	0.161	0.084	0.042	0.020	17,740
			Meta-analysis (k-means)	n/a	0.427	0.279	0.180	0.112	0.067	17,740
		LD-aware GT	Meta-analysis	n/a	0.019	3.1x10 <sup>-3</sup>	5.6x10 <sup>-4</sup>	1.7x10 <sup>-4</sup>	1.1x10 <sup>-4</sup>	17,740
			Meta-analysis (k-means)	n/a	0.107	0.043	0.020	9.5x10 <sup>-3</sup>	5.0x10 <sup>-3</sup>	17,740
TOPMed	LQ	GT	Meta-analysis	n/a	0.553	0.523	0.501	0.485	0.471	329,699
			Meta-analysis (k-means)	n/a	0.557	0.526	0.505	0.488	0.474	329,699
		HQ	Meta-analysis	n/a	0.064	0.022	9.2x10 <sup>-3</sup>	5.0x10 <sup>-3</sup>	3.3x10 <sup>-3</sup>	17,524
			Meta-analysis (k-means)	n/a	0.224	0.121	0.074	0.047	0.033	17,524
	LQ	GL	RUTH-LRT	2	0.357	0.304	0.271	0.243	0.224	10,966
			RUTH-Score	4	0.358	0.306	0.270	0.243	0.225	10,966
			RUTH-LRT	2	0.336	0.293	0.263	0.241	0.221	10,966
			RUTH-Score	4	0.336	0.295	0.264	0.242	0.223	10,966
		LD-aware GT	RUTH-LRT	2	0.220	0.177	0.149	0.128	0.113	10,966
			RUTH-Score	4	0.215	0.177	0.151	0.131	0.115	10,966
			RUTH-Score	2	0.211	0.169	0.143	0.124	0.109	10,966
			RUTH-LRT	4	0.211	0.172	0.147	0.130	0.112	10,966
1000G	HQ	raw GT	RUTH-LRT	2	0.438	0.377	0.338	0.308	0.284	10,966
			RUTH-Score	4	0.431	0.373	0.335	0.305	0.28	10,966
			RUTH-Score	2	0.424	0.372	0.335	0.309	0.286	10,966
			RUTH-Score	4	0.418	0.367	0.333	0.305	0.284	10,966
		GL	RUTH-LRT	2	0.110	0.040	0.016	7.3x10 <sup>-3</sup>	3.3x10 <sup>-3</sup>	17,740
			RUTH-Score	4	0.036	6.4x10 <sup>-3</sup>	1.3x10 <sup>-3</sup>	5.1x10 <sup>-4</sup>	3.4x10 <sup>-4</sup>	17,740
			RUTH-Score	2	0.087	0.026	9.2x10 <sup>-3</sup>	3.4x10 <sup>-3</sup>	1.6x10 <sup>-3</sup>	17,740
			RUTH-LRT	4	0.026	3.3x10 <sup>-3</sup>	7.9x10 <sup>-4</sup>	4.5x10 <sup>-4</sup>	3.4x10 <sup>-4</sup>	17,740
		LD-aware GT	RUTH-LRT	2	0.041	0.014	5.4x10 <sup>-3</sup>	2.4x10 <sup>-3</sup>	1.4x10 <sup>-3</sup>	17,740
			RUTH-Score	4	0.011	1.1x10 <sup>-3</sup>	2.3x10 <sup>-4</sup>	5.6x10 <sup>-5</sup>	0	17,740
			RUTH-Score	2	0.034	9.5x10 <sup>-3</sup>	2.8x10 <sup>-3</sup>	1.2x10 <sup>-3</sup>	5.1x10 <sup>-4</sup>	17,740
			RUTH-Score	4	0.011	1.9x10 <sup>-3</sup>	1.1x10 <sup>-4</sup>	0	0	17,740
	TOPMed	raw GT	RUTH-LRT	2	0.299	0.176	0.098	0.055	0.03	17,740
			RUTH-Score	4	0.200	0.095	0.044	0.021	9.7x10 <sup>-3</sup>	17,740
			RUTH-Score	2	0.276	0.155	0.083	0.044	0.023	17,740
			RUTH-Score	4	0.183	0.083	0.036	0.015	7.4x10 <sup>-3</sup>	17,740
		GL	RUTH-LRT	2	0.646	0.610	0.584	0.563	0.547	329,699
			RUTH-Score	4	0.652	0.614	0.588	0.567	0.55	329,699
			RUTH-Score	2	0.634	0.607	0.589	0.574	0.562	329,699
			RUTH-LRT	4	0.635	0.608	0.590	0.575	0.562	329,699
	HQ	GT	RUTH-LRT	2	0.603	0.573	0.551	0.533	0.518	329,699
			RUTH-Score	4	0.610	0.580	0.556	0.538	0.552	329,699
			RUTH-Score	2	0.608	0.586	0.571	0.558	0.548	329,699
			RUTH-Score	4	0.608	0.587	0.572	0.559	0.549	329,699
		GL	RUTH-LRT	2	0.130	0.067	0.039	0.024	0.016	17,524
			RUTH-Score	4	0.041	0.018	8.7x10 <sup>-3</sup>	4.2x10 <sup>-3</sup>	3.1x10 <sup>-3</sup>	17,524
			RUTH-Score	2	0.130	0.065	0.036	0.021	0.014	17,524
			RUTH-Score	4	0.034	0.011	4.9x10 <sup>-3</sup>	3.1x10 <sup>-3</sup>	2.5x10 <sup>-3</sup>	17,524
	HQ	GT	RUTH-LRT	2	0.079	0.028	0.012	7.6x10 <sup>-3</sup>	5.9x10 <sup>-3</sup>	17,524
			RUTH-Score	4	0.125	0.036	0.012	5.0x10 <sup>-3</sup>	2.7x10 <sup>-3</sup>	17,524
		GL	RUTH-Score	2	0.093	0.033	0.015	8.8x10 <sup>-3</sup>	6.0x10 <sup>-3</sup>	17,524
			RUTH-Score	4	0.145	0.047	0.017	7.1x10 <sup>-3</sup>	3.5x10 <sup>-3</sup>	17,524

1000 In both 1000G and TOPMed, the false positive rate was much higher when k-means-based groupings were used for  
 1001 meta-analysis, compared to when high quality ancestry groupings were used. Similarly, the false positive rate was  
 1002 much higher when only 2 PCs were used, compared to when 4 PCs were used. Surprisingly, in TOPMed, using 4 PCs  
 1003 led to both a lower false positive rate and higher true positive rate when compared to using 2 PCs.

1004 **Table S3**

1005 Performance of the unadjusted test, meta-analysis, and RUTH on the subset of TOPMed freeze 5 chromosome 20  
1006 variants that are also found in 1000G.

1007

Variant set	Genotype Format	HWE Test	Proportion of Significant Variants					Total Variant Count
			P < 10 <sup>-2</sup>	P < 10 <sup>-3</sup>	P < 10 <sup>-4</sup>	P < 10 <sup>-5</sup>	P < 10 <sup>-6</sup>	
HQ Variants	raw GT	Unadjusted	0.890	0.842	0.800	0.766	0.736	16,924
	raw GT	Meta-analysis	0.062	0.020	8.0x10 <sup>-3</sup>	3.8x10 <sup>-3</sup>	2.3x10 <sup>-3</sup>	16,924
	raw GT	RUTH-Score	0.145	0.046	0.016	6.3x10 <sup>-3</sup>	2.8x10 <sup>-3</sup>	16,924
	GL	RUTH-Score	0.032	9.3x10 <sup>-3</sup>	3.7x10 <sup>-3</sup>	2.0x10 <sup>-3</sup>	1.5x10 <sup>-3</sup>	16,924
	raw GT	RUTH-LRT	0.125	0.035	0.011	4.2x10 <sup>-3</sup>	1.9x10 <sup>-3</sup>	16,924
	GL	RUTH-LRT	0.039	0.016	7.4x10 <sup>-3</sup>	3.1x10 <sup>-3</sup>	2.2x10 <sup>-3</sup>	16,924
LQ Variants	raw GT	Unadjusted	0.762	0.728	0.702	0.683	0.667	10,513
	raw GT	Meta-analysis	0.649	0.616	0.592	0.575	0.560	10,513
	raw GT	RUTH-Score	0.727	0.693	0.673	0.656	0.640	10,513
	GL	RUTH-Score	0.698	0.669	0.648	0.631	0.618	10,513
	raw GT	RUTH-LRT	0.719	0.686	0.663	0.643	0.627	10,513
	GL	RUTH-LRT	0.693	0.662	0.639	0.621	0.605	10,513

1008 For HQ variants, GL-based HWE tests had much better control of false positives than GT-based tests.  
1009 Conversely, for LQ variants, GT-based HWE tests had a slightly better true positive rate than GL-based  
1010 tests. Overall, GL-based tests had the best performance when considering the tradeoff between false  
1011 positives and true positives (Figure S5-6).

1012

1013 **Table S4**

1014 Simulation results for RUTH tests using 2 vs 4 principal components.

1015 This table can be found at the following link:

1016 <https://docs.google.com/spreadsheets/d/1Ac9rveZax5Y8NIKQ47wBaJNELqeJkFuNUpa1sNgnSno/edit?usp=sharing>

1017 We tested the effect of using different numbers of PCs in RUTH on Type I Error ( $\theta = 0$ ) and power ( $\theta \neq 0$ ) for

1018 simulated samples with different numbers of ancestries, fixation indices, sequencing depths, and genotype

1019 representations. We simulated 50,000 variants for each combination of simulation parameters.

1020

1021 **Table S5**

1022 The effect of high vs. low quality subpopulation classification on meta-analysis in simulated samples.

1023

Grouping	Depth	Theta	Proportion of significant variants				
			$P < 10^{-6}$	$P < 10^{-5}$	$P < 10^{-4}$	$P < 10^{-3}$	$P < 0.01$
True ancestry labels	5	-0.05	0.0073	0.0125	0.0235	0.05	0.1145
		0	0.0147	0.0388	0.0919	0.1955	0.3519
	30	-0.05	0.0139	0.04	0.1048	0.2389	0.4594
		0	0	0	0.0001	0.0016	0.0127
k-means (3 groups)	5	-0.05	0.1201	0.149	0.19	0.2509	0.3513
		0	0.2907	0.3496	0.4195	0.4977	0.5826
	30	-0.05	0.0919	0.1122	0.1447	0.2017	0.3097
		0	0.2183	0.2553	0.3054	0.3734	0.4747

1024 We simulated 50,000 variants in 5,000 samples arising from 5 distinct subpopulations (1,000 samples each), at low  
1025 (5x) and high (30x) depth, with no deviation from HWE ( $\theta = 0$ ) and moderate excess heterozygosity ( $\theta = -0.05$ ). We  
1026 used one of two different groupings for our samples: for high-quality labels, we used the original true ancestry  
1027 labels from which we simulated our data; for low-quality labels, we ran k-means classification on the first 2  
1028 principal components of genetic variation for all our samples to generate 3 groups. We meta-analyzed all data sets  
1029 using Stouffer's method. Type I error rates for low-depth samples were greatly inflated. For high-depth samples,  
1030 when we used the true ancestry labels, Type I errors were well-controlled, with reasonable power to discover  
1031 deviations from HWE, while when we used the crude k-means labels, Type I errors were greatly inflated, with  
1032 surprisingly less power to discover deviations from HWE at less stringent P-value thresholds. These results  
1033 highlight the importance of high-quality subpopulation classification for meta-analysis.

1034

1035 **Table S6**

1036 Comparison of runtimes and memory requirements for RUTH and PCAngsd in simulated and 1000G data.

1037

Data set	Genotype Format	Software	Test	N	Total Variant Count	Runtime (s)	Memory requirement (MB)
Simulated	GT	PLINK	Unadjusted	5,000	50,000	22	10
	GT	RUTH	RUTH LRT	5,000	50,000	348	15
	GL	RUTH	RUTH LRT	5,000	50,000	341	15
	GT	RUTH	RUTH Score	5,000	50,000	460	15
	GL	RUTH	RUTH Score	5,000	50,000	469	15
Simulated (5x)	GL	PCAngsd	PCAngsd	5,000	50,000	6,068	6,946
Simulated (30x)	GL	PCAngsd	PCAngsd	5,000	50,000	5,337	6,872
1000G	GT	PLINK	Unadjusted	2,504	28,706	2	8
	GL	RUTH	RUTH LRT	2,504	28,706	147	14
	GT	RUTH	RUTH LRT	2,504	28,706	96	13
	GL	RUTH	RUTH Score	2,504	28,706	216	14
	GT	RUTH	RUTH Score	2,504	28,706	177	13
TOPMed	GL	PCAngsd	PCAngsd	2,504	28,660	4,105	2,073
	GT	RUTH	RUTH LRT	53,831	347,223	158,731	57
	GL	RUTH	RUTH LRT	53,831	347,223	196,169	57

1038 Simulation runtimes for PLINK and RUTH are averaged over 360 runs, across combinations of different simulation  
1039 parameters. Simulation results for PCAngsd are averaged over 66 runs each for 5x and 30x coverage data. The  
1040 higher uncertainty in low depth simulated data appears to have led to slower convergence in PCAngsd. All results  
1041 for 1000G were from single runs. The listed TOPMed runtimes and memory requirements are for single-threaded  
1042 analyses of all variants.

1043

1044

Table S7

TOPMed Study Name	TOPMed Accession	Sample Size
Genetics of Cardiometabolic Health in the Amish	phs000956	1,025
Trans-Omics for Precision Medicine Whole Genome Sequencing Project: ARIC	phs001211	3,585
The Genetics and Epidemiology of Asthma in Barbados	phs001143	944
Cleveland Clinic Atrial Fibrillation Study	phs001189	328
The Cleveland Family Study (WGS)	phs000954	919
Cardiovascular Health Study	phs001368	69
Genetic Epidemiology of COPD (COPDGene) in theTOPMed Program	phs000951	8,733
The Genetic Epidemiology of Asthma in Costa Rica	phs000988	1,040
Diabetes Heart Study African American Coronary Artery Calcification (AA CAC)	phs001412	322
Whole Genome Sequencing and Related Phenotypes in the Framingham Heart Study	phs000974	3,725
Genes-environments and Admixture in Latino Asthmatics (GALA II) Study	phs000920	912
GeneSTAR (Genetic Study of Atherosclerosis Risk)	phs001218	1,633
Genetic Epidemiology Network of Arteriopathy (GENOA)	phs001345	1,069
Genetic Epidemiology Network of Salt Sensitivity (GenSalt)	phs001217	1,680
Genetics of Lipid Lowering Drugs and Diet Network (GOLDN)	phs001359	892
Heart and Vascular Health Study (HVH)	phs000993	64
HyperGEN - Genetics of Left Ventricular (LV) Hypertrophy	phs001293	1,752
Jackson Heart Study	phs000964	3,074
Whole Genome Sequencing of Venous Thromboembolism (WGS of VTE)	phs001402	1,250
MESA and MESA Family AA-CAC	phs001416	4,804
MGH Atrial Fibrillation Study	phs001062	916
Partners HealthCare Biobank	phs001024	109
San Antonio Family Heart Study (WGS)	phs001215	1,478
Study of African Americans, Asthma, Genes and Environment (SAGE) Study	phs000921	450
African American Sarcoidosis Genetics Resource	phs001207	606
Genome-wide Association Study of Adiposity in Samoans	phs000972	1,198
The Vanderbilt AF Ablation Registry	phs000997	154
The Vanderbilt Atrial Fibrillation Registry	phs001032	1016
Novel Risk Factors for the Development of Atrial Fibrillation in Women	phs001040	97
Women's Health Initiative (WHI)	phs001237	9,984
Total		53,831

1045

Sample contributions from each of the participating TOPMed studies.

1046

1047

**Table S8**

TOPMed Accession #	TOPMed Project	Parent Study	TOPMed		
			Phase	Omics Center	Omics Support
phs000956	Amish	Amish	1	Broad Genomics	3R01HL121007-01S1
phs001211	AFGen	ARIC AFGen	1	Broad Genomics	3R01HL092577-06S1 3U54HG003273-12S2 / HHSN268201500015C
phs001211	VTE	ARIC	2	Baylor	3R01HL092577-06S1 3U54HG003273-12S2 / HHSN268201500015C
phs001143	BAGS	BAGS	1	Illumina	3R01HL104608-04S1
phs001189	AFGen	CCAF	1	Broad Genomics	3R01HL092577-06S1
phs000954	CFS	CFS	1	NWGC	3R01HL098433-05S1
phs000954	CFS	CFS	3.5	NWGC	HHSN268201600032I
phs001368	CHS	CHS	3	Baylor	HHSN268201600033I 3U54HG003273-12S2 / HHSN268201500015C
phs001368	VTE	CHS VTE	2	Baylor	HHSN268201500015C
phs000951	COPD	COPDGene	1	NWGC	3R01HL089856-08S1
phs000951	COPD	COPDGene	2	Broad Genomics	HHSN268201500014C
phs000951	COPD	COPDGene	2.5	Broad Genomics	HHSN268201500014C
phs000988	CRA_CAMP	CRA	1	NWGC	3R37HL066289-13S1
phs000988	CRA_CAMP	CRA	3	NWGC	HHSN268201600032I
phs001412	AA_CAC	DHS	2	Broad Genomics	HHSN268201500014C
phs000974	AFGen	FHS AFGen	1	Broad Genomics	3R01HL092577-06S1
phs000974	FHS	FHS	1	Broad Genomics	3U54HG003067-12S2
phs000920	ATGC	GALAI ATGC	3	NWGC	HHSN268201600032I
phs000920	PGX_Asthma	GALAI	1	NYGC	3R01HL117004-02S3
phs001218	AA_CAC	GeneSTAR AA_CAC	2	Broad Genomics	HHSN268201500014C
phs001218	GeneSTAR	GeneSTAR	legacy	Illumina	R01HL112064
phs001218	GeneSTAR	GeneSTAR		Psomagen	3R01HL112064-04S1
phs001345	HyperGEN_GENOA	GENOA	2	NWGC	3R01HL055673-18S1
phs001345	AA_CAC	GENOA AA_CAC	2	Broad Genomics	HHSN268201500014C
phs001217	GenSalt	GenSalt	2	Baylor	HHSN268201500015C
phs001359	GOLDN	GOLDN	2	NWGC	3R01HL104135-04S1
phs000993	AFGen	HVH	1	Broad Genomics	3R01HL092577-06S1 3U54HG003273-12S2 / HHSN268201500015C
phs000993	VTE	HVH VTE	2	Baylor	HHSN268201500015C
phs001293	HyperGEN_GENOA	HyperGEN	2	NWGC	3R01HL055673-18S1
phs000964	JHS	JHS	1	NWGC	HHSN268201100037C 3U54HG003273-12S2 / HHSN268201500015C
phs001402	VTE	Mayo_VTE	2	Baylor	HHSN268201500015C
phs001416	AA_CAC	MESA AA_CAC	2	Broad Genomics	HHSN268201500014C
phs001416	MESA	MESA	2	Broad Genomics	3U54HG003067-13S1 3U54HG003067-12S2 / 3U54HG003067-13S1; 3U54HG003067-12S2 / 3U54HG003067-13S1;
phs001062	AFGen	MGH_AF	1.4; 1.5; 2.4	Broad Genomics	3UM1HG008895-01S2
phs001062	AFGen	MGH_AF	1	Broad Genomics	3R01HL092577-06S1
phs001024	AFGen	Partners	1	Broad Genomics	3R01HL092577-06S1
phs001215	SAFS	SAFS	1	Illumina	3R01HL113323-03S1
phs001215	SAFS	SAFS	legacy	Illumina	R01HL113322
phs000921	ATGC	SAGE ATGC	3	NWGC	HHSN268201600032I
phs000921	PGX_Asthma	SAGE	1	NYGC	3R01HL117004-02S3
phs000972	Samoan	Samoan	1	NWGC	HHSN268201100037C
phs000972	Samoan	Samoan	2	NYGC	HHSN268201500016C
phs001207	Sarcoidosis	Sarcoidosis	2	Baylor	3R01HL113326-04S1
phs001207	Sarcoidosis	Sarcoidosis	3.5	NWGC	HHSN268201600032I 3U54HG003067-12S2 / 3U54HG003067-13S1; 3U54HG003067-12S2 / 3U54HG003067-13S1;
phs000997	AFGen	VAFAR	1.5; 2.4; 5.3	Broad Genomics	3UM1HG008895-01S2

phs000997	AFGen	VAFAR	1	Broad Genomics	3R01HL092577-06S1
phs001032	AFGen	VU_AF	1	Broad Genomics	3R01HL092577-06S1
phs001040	AFGen	WGHS	1	Broad Genomics	3R01HL092577-06S1
phs001237	WHI	WHI	2	Broad Genomics	HHSN268201500014C

1048 TOPMed acknowledgements for omics support.

1049

1050 **File S1**

1051 **TOPMed Study Acknowledgements**

1052 **NHLBI TOPMed: Genetics of Cardiometabolic Health in the Amish**

1053 The Amish studies upon which these data are based were supported by NIH grants R01  
1054 AG18728, U01 HL072515, R01 HL088119, R01 HL121007, and P30 DK072488. See publication:  
1055 PMID: 18440328

1056 **NHLBI TOPMed: Trans-Omics for Precision Medicine Whole Genome Sequencing Project: ARIC**

1057 Genome Sequencing for “NHLBI TOPMed: Atherosclerosis Risk in Communities (ARIC)”  
1058 (phs001211) was performed at the Baylor College of Medicine Human Genome Sequencing  
1059 Center (HHSN268201500015C and 3U54HG003273-12S2) and the Broad Institute of MIT and  
1060 Harvard (3R01HL092577-06S1).

1061 The Atherosclerosis Risk in Communities study has been funded in whole or in part with Federal  
1062 funds from the National Heart, Lung, and Blood Institute, National Institutes of Health,  
1063 Department of Health and Human Services (contract numbers HHSN268201700001I,  
1064 HHSN268201700002I, HHSN268201700003I, HHSN268201700004I and HHSN268201700005I).  
1065 The authors thank the staff and participants of the ARIC study for their important contributions.

1066 **NHLBI TOPMed: The Genetics and Epidemiology of Asthma in Barbados**

1067 The Genetics and Epidemiology of Asthma in Barbados is supported by National Institutes of  
1068 Health (NIH) National Heart, Lung, Blood Institute TOPMed (R01 HL104608-S1) and: R01  
1069 AI20059, K23 HL076322, and RC2 HL101651. For the specific cohort descriptions and  
1070 descriptions regarding the collection of phenotype data can be found at:  
1071 <https://www.ncbi.nlm.nih.gov/pmc/articles/PMC8500000/>. The authors wish to give special recognition to  
1072 the individual study participants who provided biological samples and or data, without their  
1073 support in research none of this would be possible.

1074 **NHLBI TOPMed: Cleveland Clinic Atrial Fibrillation Study**

1075 The research reported in this article was supported by grants from the National Institutes of  
1076 Health (NIH) National Heart, Lung, and Blood Institute grants R01 HL090620 and R01 HL111314,  
1077 the NIH National Center for Research Resources for Case Western Reserve University and the  
1078 Cleveland Clinic Clinical and Translational Science Award (CTSA) UL1-RR024989, the  
1079 Department of Cardiovascular Medicine philanthropic research fund, Heart and Vascular  
1080 Institute, Cleveland Clinic, the Fondation Leducq grant 07-CVD 03, and The Atrial Fibrillation  
1081 Innovation Center, State of Ohio.

1082 **NHLBI TOPMed: The Cleveland Family Study (WGS)**

1083 Support for the Cleveland Family Study was provided by NHLBI grant numbers R01 HL46380,  
1084 R01 HL113338 and R35 HL135818.

1085 **NHLBI TOPMed: Cardiovascular Health Study**

1086 This research was supported by contracts HHSN268201200036C, HHSN268200800007C,  
1087 HHSN268201800001C, N01-HC85079, N01-HC-85080, N01-HC-85081, N01-HC-85082, N01-HC-  
1088 85083, N01-HC-85084, N01-HC-85085, N01-HC-85086, N01-HC-35129, N01-HC-15103, N01-HC-  
1089 55222, N01-HC-75150, N01-HC-45133, and N01-HC-85239; grant numbers U01 HL080295, U01  
1090 HL130114 and R01 HL059367 from the National Heart, Lung, and Blood Institute, and R01  
1091 AG023629 from the National Institute on Aging, with additional contributions from the National  
1092 Institute of Neurological Disorders and Stroke. A full list of principal CHS investigators and  
1093 institutions can be found at <https://chs-nhlbi.org/pi>. Its content is solely the responsibility of  
1094 the authors and does not necessarily represent the official views of the National Institutes of  
1095 Health.

1096 **NHLBI TOPMed: Genetic Epidemiology of COPD (COPDGene) in the TOPMed Program**

1097 This research used data generated by the COPDGene study, which was supported by NIH Award  
1098 Number U01 HL089897 and Award Number U01 HL089856 from the National Heart, Lung, and  
1099 Blood Institute. The content is solely the responsibility of the authors and does not necessarily  
1100 represent the official views of the National Heart, Lung, and Blood Institute or the National  
1101 Institutes of Health.

1102 The COPDGene project is also supported by the COPD Foundation through contributions made  
1103 to an Industry Advisory Board comprised of AstraZeneca, Boehringer Ingelheim,  
1104 GlaxoSmithKline, Novartis, Pfizer, Siemens and Sunovion.

1105 **NHLBI TOPMed: The Genetic Epidemiology of Asthma in Costa Rica**

1106 This study was supported by NHLBI grants R37 HL066289 and P01 HL132825. We wish to  
1107 acknowledge the investigators at the Channing Division of Network Medicine at Brigham and  
1108 Women's Hospital, the investigators at the Hospital Nacional de Niños in San José, Costa Rica  
1109 and the study subjects and their extended family members who contributed samples and  
1110 genotypes to the study, and the NIH/NHLBI for its support in making this project possible.

1111 **NHLBI TOPMed: Diabetes Heart Study African American Coronary Artery Calcification (AA  
1112 CAC)**

1113 This work was supported by R01 HL92301, R01 HL67348, R01 NS058700, R01 AR48797, R01  
1114 DK071891, R01 AG058921, the General Clinical Research Center of the Wake Forest University  
1115 School of Medicine (M01 RR07122, F32 HL085989), the American Diabetes Association, and a  
1116 pilot grant from the Claude Pepper Older Americans Independence Center of Wake Forest  
1117 University Health Sciences (P60 AG10484).

---

1118 **NHLBI TOPMed: Whole Genome Sequencing and Related Phenotypes in the Framingham**  
1119 **Heart Study**

1120 The Framingham Heart Study (FHS) is a prospective cohort study of 3 generations of subjects  
1121 who have been followed up to 65 years to evaluate risk factors for cardiovascular disease.<sup>13-16</sup>  
1122 Its large sample of ~15,000 men and women who have been extensively phenotyped with  
1123 repeated examinations make it ideal for the study of genetic associations with cardiovascular  
1124 disease risk factors and outcomes. DNA samples have been collected and immortalized since  
1125 the mid-1990s and are available on ~8000 study participants in 1037 families. These samples  
1126 have been used for collection of GWAS array data and exome chip data in nearly all with DNA  
1127 samples, and for targeted sequencing, deep exome sequencing and light coverage whole  
1128 genome sequencing in limited numbers. Additionally, mRNA and miRNA expression data, DNA  
1129 methylation data, metabolomics and other 'omics data are available on a sizable portion of  
1130 study participants. This project will focus on deep whole genome sequencing (mean 30X  
1131 coverage) in ~4100 subjects and imputed to all with GWAS array data to more fully understand  
1132 the genetic contributions to cardiovascular, lung, blood and sleep disorders.

1133 The FHS acknowledges the support of contracts NO1-HC-25195 and HHSN268201500001I from  
1134 the National Heart, Lung, and Blood Institute and grant supplement R01 HL092577-06S1 for this  
1135 research. We also acknowledge the dedication of the FHS study participants without whom this  
1136 research would not be possible.

1137 **NHLBI TOPMed: Genes-environments and Admixture in Latino Asthmatics (GALA II) Study**

1138 The Genes-environments and Admixture in Latino Americans (GALA II) Study was supported by  
1139 the National Heart, Lung, and Blood Institute of the National Institute of Health (NIH) grants  
1140 R01HL117004 and X01HL134589; study enrollment supported by the Sandler Family  
1141 Foundation, the American Asthma Foundation, the RWJF Amos Medical Faculty Development  
1142 Program, Harry Wm. and Diana V. Hind Distinguished Professor in Pharmaceutical Sciences II  
1143 and the National Institute of Environmental Health Sciences grant R01ES015794.

1144  
1145 The GALA II study collaborators include Shannon Thyne, UCSF; Harold J. Farber, Texas Children's  
1146 Hospital; Denise Serebrisky, Jacobi Medical Center; Rajesh Kumar, Lurie Children's Hospital of  
1147 Chicago; Emerita Brigino-Buenaventura, Kaiser Permanente; Michael A. LeNoir, Bay Area  
1148 Pediatrics; Kelley Meade, UCSF Benioff Children's Hospital, Oakland; William Rodriguez-Cintron,  
1149 VA Hospital, Puerto Rico; Pedro C. Avila, Northwestern University; Jose R. Rodriguez-Santana,  
1150 Centro de Neumologia Pediatrica; Luisa N. Borrell, City University of New York; Adam Davis,  
1151 UCSF Benioff Children's Hospital, Oakland; Saunak Sen, University of Tennessee and Fred  
1152 Lurmann, Sonoma Technologies, Inc.

1153  
1154 The authors acknowledge the families and patients for their participation and thank the  
1155 numerous health care providers and community clinics for their support and participation in  
1156 GALA II. In particular, the authors thank study coordinator Sandra Salazar; the recruiters who  
1157 obtained the data: Duanny Alva, MD, Gaby Ayala-Rodriguez, Lisa Caine, Elizabeth Castellanos,  
1158 Jaime Colon, Denise DeJesus, Blanca Lopez, Brenda Lopez, MD, Louis Martos, Vivian Medina,  
1159 Juana Olivo, Mario Peralta, Esther Pomares, MD, Jihan Quraishi, Johanna Rodriguez, Shahdad

1160 Saeedi, Dean Soto, Ana Taveras; and the lab researcher Celeste Eng who processed the  
1161 biospecimens.  
1162

1163 **NHLBI TOPMed: Genetic Epidemiology Network of Arteriopathy (GENOA)**

1164 Support for GENOA was provided by the National Heart, Lung and Blood Institute (HL054457,  
1165 HL054464, HL054481, HL119443, and HL087660) of the National Institutes of Health. WGS for  
1166 “NHLBI TOPMed: Genetic Epidemiology Network of Arteriopathy” (phs001345) was performed  
1167 at the Mayo Clinic Genotyping Core, the DNA Sequencing and Gene Analysis Center at the  
1168 University of Washington (3R01HL055673-18S1), and the Broad Institute  
1169 (HHSN268201500014C) for their genotyping and sequencing services. We would like to thank  
1170 the GENOA participants.

1171 **NHLBI TOPMed: Genetic Epidemiology Network of Salt Sensitivity (GenSalt)**

1172 The Genetic Epidemiology Network of Salt-Sensitivity (GenSalt) was supported by research  
1173 grants (U01HL072507, R01HL087263, and R01HL090682) from the National Heart, Lung, and  
1174 Blood Institute, National Institutes of Health, Bethesda, MD.

1175 **NHLBI TOPMed: Genetics of Lipid Lowering Drugs and Diet Network (GOLDN)**

1176 GOLDN biospecimens, baseline phenotype data, and intervention phenotype data were  
1177 collected with funding from the National Heart, Lung and Blood Institute (NHLBI) grant U01  
1178 HL072524. Whole-genome sequencing in GOLDN was funded by NHLBI grant R01 HL104135 and  
1179 supplement R01 HL104135-04S1.

1180 **NHLBI TOPMed: Heart and Vascular Health Study (HVH)**

1181 The research reported in this article was supported by grants HL068986, HL085251, HL095080,  
1182 and HL073410 from the National Heart, Lung, and Blood Institute.

1183 **NHLBI TOPMed: Hypertension Genetic Epidemiology Network (HyperGEN)**

1184 The HyperGEN Study is part of the National Heart, Lung, and Blood Institute (NHLBI) Family  
1185 Blood Pressure Program; collection of the data represented here was supported by grants U01  
1186 HL054472 (MN Lab), U01 HL054473 (DCC), U01 HL054495 (AL FC), and U01 HL054509 (NC FC).  
1187 The HyperGEN: Genetics of Left Ventricular Hypertrophy Study was supported by NHLBI grant  
1188 R01 HL055673 with whole-genome sequencing made possible by supplement -18S1.

1189 **NHLBI TOPMed: The Jackson Heart Study**

1190 The Jackson Heart Study (JHS) is supported and conducted in collaboration with Jackson State  
1191 University (HHSN268201800013I), Tougaloo College (HHSN268201800014I), the Mississippi  
1192 State Department of Health (HHSN268201800015I/HHSN26800001) and the University of  
1193 Mississippi Medical Center (HHSN268201800010I, HHSN268201800011I and

1194 HHSN268201800012I) contracts from the National Heart, Lung, and Blood Institute (NHLBI) and  
1195 the National Institute for Minority Health and Health Disparities (NIMHD). The authors also  
1196 wish to thank the staffs and participants of the JHS.

1197 **NHLBI TOPMed: Multi-Ethnic Study of Atherosclerosis**

1198 MESA and the MESA SHARe projects are conducted and supported by the National Heart, Lung,  
1199 and Blood Institute (NHLBI) in collaboration with MESA investigators. Support for MESA is  
1200 provided by contracts 75N92020D00001, HHSN268201500003I, N01-HC-95159,  
1201 75N92020D00005, N01-HC-95160, 75N92020D00002, N01-HC-95161, 75N92020D00003, N01-  
1202 HC-95162, 75N92020D00006, N01-HC-95163, 75N92020D00004, N01-HC-95164,  
1203 75N92020D00007, N01-HC-95165, N01-HC-95166, N01-HC-95167, N01-HC-95168, N01-HC-  
1204 95169, UL1-TR-000040, UL1-TR-001079, and UL1-TR-001420. Also supported by the National  
1205 Center for Advancing Translational Sciences, CTSI grant UL1TR001881, and the National  
1206 Institute of Diabetes and Digestive and Kidney Disease Diabetes Research Center (DRC) grant  
1207 DK063491 to the Southern California Diabetes Endocrinology Research Center.

1208 **NHLBI TOPMed: Whole Genome Sequencing of Venous Thromboembolism (WGS of VTE)**

1209 Funded in part by grants from the National Institutes of Health, National Heart, Lung, and Blood  
1210 Institute (HL66216 and HL83141) and the National Human Genome Research Institute  
1211 (HG04735).

1212 **NHLBI TOPMed: MGH Atrial Fibrillation Study**

1213 This work was supported by the Fondation Leducq (14CVD01), and by grants from the National  
1214 Institutes of Health to Dr. Ellinor (1R01HL092577, R01HL128914, K24HL105780). This work was  
1215 also supported by a grant from the American Heart Association to Dr. Ellinor  
1216 (18SFRN34110082). Dr. Lubitz is supported by NIH grant 1R01HL139731 and AHA  
1217 18SFRN34250007.

1218 **NHLBI TOPMed: Partners HealthCare Biobank**

1219 We thank the Broad Institute for generating high-quality sequence data supported by the NHLBI  
1220 grant 3R01HL092577-06S1 to Dr. Patrick Ellinor. The datasets used in this manuscript were  
1221 obtained from dbGaP at <http://www.ncbi.nlm.nih.gov/gap> through dbGaP accession number  
1222 phs001024.

1223 **NHLBI TOPMed: Study of African Americans, Asthma, Genes and Environment (SAGE)**

1224 The Study of African Americans, Asthma, Genes and Environments (SAGE) was supported by the  
1225 National Heart, Lung, and Blood Institute of the National Institute of Health (NIH) grants  
1226 R01HL117004 and X01HL134589; study enrollment supported by the Sandler Family  
1227 Foundation, the American Asthma Foundation, the RWJF Amos Medical Faculty Development  
1228 Program, Harry Wm. and Diana V. Hind Distinguished Professor in Pharmaceutical Sciences II.

1229 The SAGE study collaborators include Harold J. Farber, Texas Children's Hospital; Emerita  
1230 Brigino-Buenaventura, Kaiser Permanente; Michael A. LeNoir, Bay Area Pediatrics; Kelley  
1231 Meade, UCSF Benioff Children's Hospital, Oakland; Luisa N. Borrell, City University of New York;  
1232 Adam Davis, UCSF Benioff Children's Hospital, Oakland and Fred Lurmann, Sonoma  
1233 Technologies, Inc.

1234 The authors acknowledge the families and patients for their participation and thank the  
1235 numerous health care providers and community clinics for their support and participation in  
1236 SAGE. In particular, the authors thank study coordinator Sandra Salazar; the recruiters who  
1237 obtained the data: Lisa Caine, Elizabeth Castellanos, Brenda Lopez, MD, Shahdad Saeedi; and  
1238 the lab researcher Celeste Eng who processed the biospecimens.

1239 E.G.B was supported by National Heart, Lung, and Blood Institute (NHLBI): U01HL138626,  
1240 R01HL117004, R01HL128439, R01HL135156, X01HL134589, R01HL141992, R01HL141845; the  
1241 National Human Genome Research Institute (NHGRI): U01HG009080; the National Institute of  
1242 Environmental Health Sciences (NIEHS): R01ES015794, R21ES24844; the National Institute on  
1243 Minority Health and Health Disparities (NIMHD): P60MD006902, R01MD010443,  
1244 RL5GM118984, R56MD013312; the Eunice Kennedy Shriver National Institute of Child Health  
1245 and Human Development (NICHD): R01HD085993; and the Tobacco-Related Disease Research  
1246 Program (TRDRP): 24RT-0025 and 27IR-0030.

#### 1247 **NHLBI TOPMed: San Antonio Family Heart Study (WGS)**

1248 Collection of the San Antonio Family Study data was supported in part by National Institutes of  
1249 Health (NIH) grants R01 HL045522, MH078143, MH078111 and MH083824; and whole genome  
1250 sequencing of SAFS subjects was supported by U01 DK085524 and R01 HL113323. We are very  
1251 grateful to the participants of the San Antonio Family Study for their continued involvement in  
1252 our research programs.

#### 1253 **NHLBI TOPMed: The Samoan Obesity, Lifestyle and Genetic Adaptations Study (OLaGA) Group**

1254 Financial support for the Samoan Obesity, Lifestyle and Genetic Adaptations Study (OLaGA)  
1255 Group comes from the U.S. National Institutes of Health Grant R01-HL093093 and R01-  
1256 HL133040. We acknowledge the assistance of the Samoa Ministry of Health and the Samoa  
1257 Bureau of Statistics for their guidance and support in the conduct of this study. We thank the  
1258 local village officials for their help and the participants for their generosity. The following  
1259 publication describes the origin of the dataset: Hawley NL, Minster RL, Weeks DE, Viali S,  
1260 Reupena MS, Sun G, Cheng H, Deka R, McGarvey ST. Prevalence of Adiposity and Associated  
1261 Cardiometabolic Risk Factors in the Samoan Genome-Wide Association Study. Am J Human Biol  
1262 2014. 26: 491-501. DOI: 10.1002/jhb.22553. PMID: 24799123.

1263 Our study name: 'The Samoan Obesity, Lifestyle and Genetic Adaptations Study (OLaGA)  
1264 Group'.

1265 Ranjan Deka, Department of Environmental and Public Health Sciences, College of Medicine,  
1266 University of Cincinnati, Cincinnati, OH 45267-0056. email: [dekar@uc.edu](mailto:dekar@uc.edu).

1267 Nicola L Hawley, Department of Epidemiology (Chronic Disease), School of Public Health, Yale  
1268 University, New Haven, CT 06520-0834. email: [nicola.hawley@yale.edu](mailto:nicola.hawley@yale.edu).

1269 Stephen T McGarvey, International Health Institute, Department of Epidemiology, School of  
1270 Public Health, and Department of Anthropology, Brown University. 02912. email:  
1271 [stephen\\_mcgarvey@brown.edu](mailto:stephen_mcgarvey@brown.edu).

1272 Ryan L Minster, Department of Human Genetics and Department of Biostatistics, University of  
1273 Pittsburgh, Pittsburgh, PA 15261. email: [rminster@pitt.edu](mailto:rminster@pitt.edu).

1274 Take Naseri, Ministry of Health, Government of Samoa, Apia, Samoa. Email:  
1275 [taken@health.gov.ws](mailto:taken@health.gov.ws).

1276 Muagututia Sefuiva Reupena, Lutia I Puava Ae Mapu I Fagalele, Apia, Samoa. Email:  
1277 [smuagututia51@gmail.com](mailto:smuagututia51@gmail.com).

1278 Daniel E Weeks, Department of Human Genetics and Department of Biostatistics, University of  
1279 Pittsburgh, Pittsburgh, PA 15261. email: [weeks@pitt.edu](mailto:weeks@pitt.edu).

## 1280 **NHLBI TOPMed: The Vanderbilt AF Ablation Registry**

1281 The research reported in this article was supported by grants from the American Heart  
1282 Association to Dr. Shoemaker (11CRP742009), Dr. Darbar (EIA 0940116N), and grants from the  
1283 National Institutes of Health (NIH) to Dr. Darbar (R01 HL092217), and Dr. Roden (U19 HL65962,  
1284 and UL1 RR024975). The project was also supported by a CTSA award (UL1 TR00045) from the  
1285 National Center for Advancing Translational Sciences. Its contents are solely the responsibility  
1286 of the authors and do not necessarily represent the official views of the National Center for  
1287 Advancing Translational Sciences or the NIH.

## 1288 **NHLBI TOPMed: The Vanderbilt Atrial Fibrillation Registry**

1289 The research reported in this article was supported by grants from the American Heart  
1290 Association to Dr. Darbar (EIA 0940116N), and grants from the National Institutes of Health  
1291 (NIH) to Dr. Darbar (HL092217), and Dr. Roden (U19 HL65962, and UL1 RR024975). This project  
1292 was also supported by CTSA award (UL1TR000445) from the National Center for Advancing  
1293 Translational Sciences. Its contents are solely the responsibility of the authors and do not  
1294 necessarily represent the official views of the National Center for Advancing Translational  
1295 Sciences of the NIH.

## 1296 **NHLBI TOPMed: Novel Risk Factors for the Development of Atrial Fibrillation in Women**

1297 The Women's Genome Health Study (WGHS) is supported by HL 043851 and HL099355 from  
1298 the National Heart, Lung, and Blood Institute and CA 047988 from the National Cancer Institute,  
1299 the Donald W. Reynolds Foundation with collaborative scientific support and funding for  
1300 genotyping provided by Amgen. AF endpoint confirmation was supported by HL-093613 and a  
1301 grant from the Harris Family Foundation and Watkin's Foundation.

## 1302 **NHLBI TOPMed: Women's Health Initiative (WHI)**

1303 The WHI program is funded by the National Heart, Lung, and Blood Institute, National Institutes  
1304 of Health, U.S. Department of Health and Human Services through contracts  
1305 HHSN268201600018C, HHSN268201600001C, HHSN268201600002C, HHSN268201600003C,  
1306 and HHSN268201600004C.

1307 **NHLBI TOPMed: GeneSTAR (Genetic Study of Atherosclerosis Risk)**

1308 The Johns Hopkins Genetic Study of Atherosclerosis Risk (GeneSTAR) was supported by grants  
1309 from the National Institutes of Health through the National Heart, Lung, and Blood Institute  
1310 (U01HL72518, HL087698, HL112064) and by a grant from the National Center for Research  
1311 Resources (M01-RR000052) to the Johns Hopkins General Clinical Research Center. We would  
1312 like to thank the participants and families of GeneSTAR and our dedicated staff for all their  
1313 sacrifices.

1314 **NHLBI TOPMed: Genetics of Sarcoidosis in African Americans (Sarcoidosis)**

1315 National Institutes of Health (R01HL113326, P30 GM110766-01)